Local remodeling of synthetic extracellular matrix microenvironments by co-cultured endometrial epithelial and stromal cells enables long-term dynamic physiological function

Citation: Cook, Christi D., Abby S. Hill, Margaret Guo, Linda Stockdale, Julia P. Papps, Keith B. Isaacson, Douglas A. Lauffenburger, and Linda G. Griffith. "Local Remodeling of Synthetic Extracellular Matrix Microenvironments by Co-Cultured Endometrial Epithelial and Stromal Cells Enables Long-Term Dynamic Physiological Function." Integrative Biology 9, no. 4 (2017): 271–289.

As Published: http://dx.doi.org/10.1039/C6IB00245E

Publisher: Royal Society of Chemistry (RSC)

Persistent URL: http://hdl.handle.net/1721.1/117608

Version: Author's final manuscript: final author's manuscript post peer review, without publisher's formatting or copy editing

HHS Public Access

Author manuscript

Integr Biol (Camb). Author manuscript; available in PMC 2018 April 18.

Published in final edited form as:

Integr Biol (Camb). 2017 April 18; 9(4): 271–289. doi:10.1039/c6ib00245e.

Local Remodeling of Synthetic Extracellular Matrix Microenvironments by Co-cultured Endometrial Epithelial and Stromal Cells Enables Long-term Dynamic Physiological Function

Christi D. Cook[1,2], **Abby S. Hill**[1,2], **Margaret Guo**[1], **Linda Stockdale**[2], **Julia P. Papps**[2], **Keith B. Isaacson**[2,6], **Douglas A. Lauffenburger**[1,2,3,4], and **Linda G. Griffith**[1,2,5]

[1]Department of Biological Engineering, Massachusetts Institute of Technology, Cambridge, MA

[2]Center for Gynepathology Research, Massachusetts Institute of Technology, Cambridge, MA

[3]Department of Biology, Massachusetts Institute of Technology, Cambridge, MA

[4]Department of Chemical Engineering, Massachusetts Institute of Technology, Cambridge, MA

[5]Department of Mechanical Engineering, Massachusetts Institute of Technology, Cambridge, MA

[6]Harvard Medical School and Center for Minimally Invasive Gynecologic Surgery, Newton Wellesley Hospital, Newton, MA

Abstract

Mucosal barrier tissues, comprising a layer of tightly-bonded epithelial cells in intimate molecular communication with an underlying matrix-rich stroma containing fibroblasts and immune cells, are prominent targets for drugs against infection, chronic inflammation, and other disease processes. Although human *in vitro* models of such barriers are needed for mechanistic studies and drug development, differences in extracellular matrix (ECM) needs of epithelial and stromal cells hinder efforts to create such models. Here, using the endometrium as an example mucosal barrier, we describe a synthetic, modular ECM hydrogel suitable for 3D functional co-culture, featuring components that can be remodeled by cells and that respond dynamically to sequester local cell-secreted ECM characteristic of each cell type. The synthetic hydrogel combines peptides with off-the-shelf reagents and is thus accessible to cell biology labs. Specifically, we first identified a single peptide as suitable for initial attachment of both endometrial epithelial and stromal cells using a 2D semi-empirical screen. Then, using a co-culture system of epithelial cells cultured on top of gel-encapsulated stromal cells, we show that inclusion of ECM-binding peptides in the hydrogel, along with the integrin-binding peptide, leads to enhanced accumulation of basement membrane beneath the epithelial layer and more fibrillar collagen matrix assembly by stromal cells over two weeks in culture. Importantly, endometrial co-cultures composed of either cell lines or primary cells displayed hormone-mediated differentiation as assessed by morphological changes and secretory protein production. A multiplex analysis of apical cytokine and growth

IRB approval

Participants were recruited through Newton-Wellesley Hospital and provided informed consent in accordance with an IRB protocol approved by the Partners Human Research Committee, and samples were analyzed at MIT in accordance with a protocol approved by the Massachusetts Institute of Technology Committee on the Use of Humans as Experimental Subjects.

factor secretion comparing cell lines and primary cells revealed strikingly different patterns, underscoring the importance of using primary cell models in analysis of cell-cell communication networks. In summary, we define a “one-size-fits-all” synthetic ECM that enables long-term, physiologically responsive co-cultures of epithelial and stromal cells in a mucosal barrier format.

TOC Image

Synthetic 3D matrix, that binds cell-secreted matrix, recapitulates endometrial physiologic epithelial-stromal tissue architecture, hormone responsiveness, and known cytokine production.

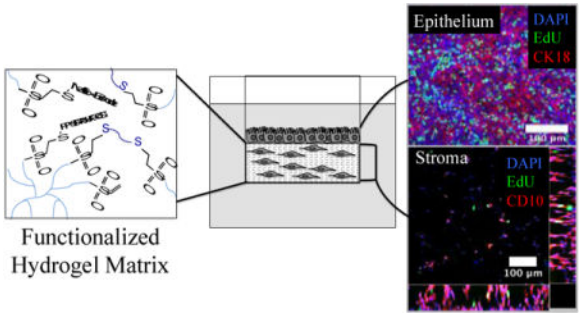

Keywords

Cell encapsulation; Hydrogel; Co-culture; ECM; Matrix binding

1. Introduction

Mucosal barrier tissues, including the digestive, respiratory and urogenital tracts, comprise a polarized, mucus-secreting epithelium that resides on top of an extracellular matrix (ECM)-rich stroma containing fibroblasts and immune cells. These barriers are the sites of complex paracrine communication events that govern tissue homeostasis, including host-microbiome interactions, as well as response to environmental insults, injury, and infection. Perturbations of barrier function are associated with both acute and chronic diseases, including Crohn’s disease, susceptibility to HIV infection, infertility, and many more.[1–5] The tremendous need to understand mucosal barrier function and assess efficacy of therapies directed at mucosal barrier diseases is driving development of both new animal models and new methods to culture human tissues to capture complex *in vivo* physiology *in vitro*. Here, using the endometrium as a model system, we establish a workflow for engineering a modular synthetic ECM scaffold that supports a functionally viable *in vitro* epithelial barrier co-culture for at least two weeks.

Several *in vitro* culture approaches have been used to analyze barrier epithelial-stromal interactions and discern integrated epithelial-stromal phenotypic responses to perturbations. At one extreme, human tissue explants can maintain crucial phenotypic functions in culture for at least days and in some cases weeks.[6,7] However, human tissue explants are not widely available, exhibit significant donor variability, cannot be readily cryopreserved for repeated studies, and require specialized culture apparatus for analysis of vectorial production of cell products. Physiologic tissue mimics created from primary cells isolated and purified from

tissues, or from cell lines, offer potential advantages of reproducibility within and between labs, and control over cell composition. Transwell-type membrane cultures are widely used, as they foster a well-polarized and well-differentiated epithelial layer that communicates with stroma plated on the underside of the semi-permeable membrane or on the bottom of the culture dish.[8–12] While this approach allows analysis of apical and basal compartments separately, it potentially distorts physiological interactions by physically separating cells and diluting paracrine signals. These latter limitations can arguably be overcome, and a more physiological 3D environment for the stromal cells created, by encapsulating stromal cells within a hydrogel ECM and plating the epithelial cells on top to engineer a better representation of normal, *in vivo* tissue architecture.

Epithelia and stroma experience different ECM environments *in vivo*. Hence, defining an appropriate ECM hydrogel for engineering mucosal barrier tissues for extended *in vitro* culture and function is an ongoing challenge. In epithelial monocultures, the basement membrane extract Matrigel™ is commonly used,[13,14] whereas type I collagen gels or fibrin gels are used as representative microenvironments for stromal cells,[15–17] with no single composition ideal for both cell types in co-culture. Further, although these and other natural ECM gels are readily available commercially, they exhibit substantial inherent batch-to-batch variability, variations in growth factor composition depending on preparation method, limited opportunity to tailor matrix degradation or signaling properties, and are difficult to microfabricate for organs-on-chips type applications.[18] In contrast, synthetic ECM can be built up in modular fashion from individual well-defined components to control crosslinking, signaling, degradation, cell adhesion, permeability, and mechanical properties in a systematic manner.[19–28] The design principles for how to tailor synthetic ECM for specific applications are still emerging, and suitable design principles for construction of a “one-size-fits-all” synthetic ECM for 3D co-culture of epithelial and stromal cells have not yet been developed.

Here, using the human endometrium as a model mucosal epithelial barrier and the well-established platform of peptide-modified PEG hydrogels crosslinked by Michael-type addition reaction,[19,20] we explore both the canonical modular synthetic ECM parameter space (crosslink density, degradation properties, adhesion ligand motifs and concentration) and identify a new design element—localized stabilization of cell-secreted matrix—that leads to phenotypically appropriate 3D tissues that are hormonally responsive over two weeks in culture. This approach incorporates features that allow initial peptide cues provided by the synthetic ECM to foster culture establishment, with additional matrix-responsive elements to reinforce cell remodeling of the microenvironment toward a tissue-appropriate architecture. A workflow for the establishment of epithelial barrier models was developed for an endometrial model, in which we (1) identified an appropriate attachment environment for stromal and epithelial cells, (2) tuned matrix remodeling by modulating extent of crosslinking and inclusion of matrix-binding peptides, (3) analyzed cell viability and function, and (4) replicated known hormone-mediated cell communication.

2. Materials and Methods

2.0. Materials

PEG macromers (40 kDa, 8-arm) functionalized with vinyl sulfone (PEG-VS) were obtained from JenKem Technology (Beijing). All peptides were custom synthesized and purified (>95%) by Boston Open Labs (Cambridge, MA). Peptides used in these studies include the following: "*MMP-CL*," a dithiol crosslinking peptide containing a matrix metalloproteinase (MMP)-sensitive substrate, (Ac)GCRD-GPQGIAGQ-DRCG(Am);[21] "*RGD*," a fibronectin (FN)-derived adhesion peptide containing the canonical RGD motif from the 10th FN type III domain NH_2-GCRE-RGDSP(Am);[20] "*PHSRN-K-RGD*," a fibronectin-derived adhesion peptide containing both the RGD motif and the PHSRN synergy site from the 9th FN Type III repeat in a branched configuration to mimic features of the biophysical presentation in FN, (Ac)PHSRNGGGK-(Ac)GGGERCG-GGRGDSPY(Am);[23,29] "*PHSRN-K-RDG*," a scrambled control sequence where the RGD motif was scrambled reducing integrin binding; (Ac)PHSRNGGGK-GGGERCG(Ac)-GGRDGSPY(Am); "*GFOGER*," a collagen I-derived adhesion peptide, NH_2-GGYGGGPG$(GPP)_5$GFOGER$(GPP)_5$GPC(Am),[30] "*Lam-5*," a laminin 5-derived adhesion peptide, NH_2-GCRG-PPFLMLLKGSTR(Am) (Lam5);[31] "*FN-binder*," a peptide with affinity for FN, (NH2-)GCRE-TLQPVYEYMVGV(-COOH);[32] and "*BM-binder*," a peptide with affinity for basement membrane proteins type IV collagen and laminin, NH_2-GCRE-ISAFLGIPFAEPPMGPRRFLPPEPKKP(Am).[33] For reactions, peptides were reconstituted in Milli-Q water (Millipore) at a concentration of 10 mM for adhesion and matrix binding peptides and 45 mM for *MMP-CL*. All other reagents and supplies were obtained as indicated in subsequent sections.

2.1 Cell culture

Ishikawa human endometrial adenocarcinoma cells (Sigma-Aldrich),[34,35] hTERT-immortalized human endometrial stromal cells (tHESCs) (ATCC),[36] and primary isolated endometrial stromal and epithelial cells were routinely cultured in a humidified atmosphere at 37°C and 5% CO_2 in phenol red-free DMEM/F12 (mixture of Dulbecco's Modified Eagle's Medium and Ham's F-12 (Gibco) media) supplemented with 1% penicillin/streptomycin (Gibco) and 10% *v*/*v* dextran/charcoal treated fetal bovine serum (Atlanta Biologicals) (DMEM/F12/FBS). Epithelial cells were split 1:4 and stromal cells were split 1:2 once they reached 70–80% confluencey, and medium was replaced every 2–3 days. Following reports of possible contamination of endometrial cell lines by HeLa or other lines,[37] STR profiling analysis (Genetic Resources Core Facility, Johns Hopkins School of Medicine, Institute of Genetic Medicine) was used to confirm the fidelity of the tHESCs and Ishikawa cell lines against known cell databanks. Cell lines were routinely used prior to passage 10 and primary cells prior to passage 4.

2.2. Primary Endometrial Cell Isolation and Expansion

Purified endometrial glandular epithelium and stromal fibroblasts were isolated from proliferative phase eutopic endometrial biopsies using established protocols as described by Osteen and co-workers[38] with some modifications (Supplementary Information). Pipelle biopsies (2 or 3 biopsies per donor) were obtained from women undergoing laparoscopic surgery for non-malignant gynecologic indications. All participants provided informed

consent in accordance with a protocol approved by the Partners Human Research Committee and the Massachusetts Institute of Technology Committee on the Use of Humans as Experimental Subjects. Study enrollment was limited to pre-menopausal women with regular cycles (26–35 days) and excluded patients with an irregular or ambiguous cycle history or a history of hormone use in the prior 3 months. All specimens were from the menstrual/proliferative phase (day 1–14) according to the donor's menstrual history (Table S1). A standardized questionnaire was used to document all clinical data.

Stromal cells were expanded in culture by seeding initial isolates (typical yield 1–5 × 10^6 cells per patient) into a T-25 or T-75 flask (Falcon) at a cell density of 2–5 × 10^4 cells/cm^2 in 4 mL or 8 mL of DMEM/F12/FBS, respectively. Cultures were grown to 80% confluencey then subcultured 1:2. Stocks were frozen at passage 2 in DMEM/F12/FBS 10% v/v DMSO (Sigma) with typical yields of 5 × 10^6 cells per patient, and 5 × 10^5 cells/vial. Freshly isolated epithelial cell glands were seeded as glandular fragments at an overall density of 0.2–2 × 10^6 cells per T-75 flask (Falcon). Epithelial cell density was confirmed prior to seeding by trypsinization and counting a portion of the glandular fraction. Stromal cells were maintained for up to two weeks prior to cryopreservation. For primary co-cultures, epithelial and stromal cells were used within one week of being freshly isolated. Primary endometrial cells from six different donors in the proliferative phase were used for these studies.

2.3. PEG hydrogel synthetic matrix

Michael-type polymerized PEG hydrogels (5 wt/wt%) were fabricated using 40 kDa 8-arm PEG-VS functionalized with cell adhesion and matrix-binding peptides. Peptide-functionalized PEG macromers, "fPEG-VS," were synthesized by incubating peptides with PEG-VS in 1× PBS, 1M HEPES (pH 7.8) buffer for 30 minutes to create macromers with 20% of the -VS groups functionalized with peptide (2 mM final concentration), with greater than 99% peptide incorporation, as assessed by Ellman's reaction, occurring after 30 minutes. The fPEG-VS solution was crosslinked with *MMP-CL*, adjusted to pH 7.8 with 1M NaOH just prior to addition, in a 0.4 thiol:VS ratio (unless otherwise noted). The concentration of free cysteine thiols was quantified utilizing Ellman's reagent (Sigma).

2D attachment studies—Attachment was assessed for tHESCs and Ishikawa cells plated on PEG hydrogels (synthesized as described above) functionalized with adhesion peptides (*RGD*, *PHSRN-K-RGD*, *GFOGE*R, or *Lam5*) at nominal concentrations of 0.25, 0.5, or 1.0 mM. The final gel solution was pipetted into 96-well angiogenesis plates (IBIDI) at 10 μL per well. Gelation proceeded for 15 minutes. Gels were then incubated in 70 μL of serum-free DMEM/F12 medium supplemented with 1% penicillin/streptomycin (DMEM/F12) overnight (5% CO2, 95% air, 37 °C), where they swelled ~2-fold in volume as measured by an increase in hydrogel mass. Cells were seeded at 4 × 10^5 cells/cm^2 in full-serum medium (DMEM/F12/FBS) at 50 μL per well. After a 6 h attachment period, wells were rinsed 2× with PBS (Ca++ and Mg++), fixed in 4% paraformaldehyde for 30 minutes at room temperature and stained with DAPI. Wells were imaged using a Leica DMI 6000 microscope and Oasis Surveyor software. Images were binarized, and DAPI-stained cell nuclei were

counted using ImageJ64 software. Attachment values were normalized to cell attachment in wells without a hydrogel.

3D stromal encapsulation—Hydrogels were fabricated on top of the membrane of Transwell inserts (Corning #3470, 6.5 mm diameter, 0.4 um pores, 0.33 cm^2 culture area, polyester) using Michael-type reaction chemistry. For these experiments, fPEG-VS macromers were prepared by reacting 8-arm PEG-VS (1.4 mM) with free thiols (-SH) on adhesion and/or matrix stabilization peptides in 1× PBS with 1 M HEPES (pH 7.8) for 30 minutes. Immediately after the functionalization reaction, the fPEG-VS macromer (average 6.4 free -VS groups per macromer) solution was mixed with a cell suspension (4.2×10^7 cells/mL in serum-free DMEM/F12, 1% penicillin/streptomycin). fPEG-VS macromers were then reacted with the cysteine thiol (-SH) groups on the bifunctional *MMP-CL* crosslinker in volumetric ratios of 8.6:1:0.4 fPEG-VS:cells:*MMP-CL* to yield a final crosslinking solution comprising 4.2×10^6 cell/mL (~50,000 cells in 12 μL), 2 mM total adhesion/matrix binding peptide, 1.2 mM total fPEG-VS macromers (5 wt%), and 1.9 mM crosslinking peptide *MMP-CL* in PBS, 1 M HEPES buffer (pH 7.8). Nominal peptide concentrations in the final gel were 1 mM *PHSRN-K-RGD*, 0.5 mM *FN-binder* and 0.5 mM *BM-binder* unless otherwise noted.

Hydrogel gelation, as determined by the point at which the solution could no longer be pipetted, occurred approximately 8 minutes (pH 7.8) after crosslinker addition, but varied between 8–12 minutes depending on the specific hydrogel formulation. The hydrogel solution was pipetted for 2 minutes to keep stromal cells in suspension, allowed to sit in tube for 3–7 minutes (where wait time = gelation time – 5 minutes), was transferred to inserts (12 μL/insert), manually spread with a pipette tip, then was centrifuged for 4 minutes at (330 RCF in an Eppendorf centrifuge 5810) to ensure gelation occurred in the middle of centrifugation creating a flat, meniscus-free hydrogel on top of the cell culture inserts. Plates were then incubated an additional 10 minutes at RT to allow crosslinking to proceed to completion. After gelation was complete, DMEM/F12/FBS was added to the apical (top) (100 μL) and basolateral (bottom) (600 μL) sides of the Transwell to achieve hydrostatic equilibrium. Cultures were maintained in a humidified incubator at 37 °C, 95% air, 5% CO_2.

Endometrial epithelial cell cultures on synthetic hydrogels with encapsulated stroma—Endometrial epithelial cells were seeded on top of gel-encapsulated stromal cells 24 h after initiation of stromal cultures. Ishikawa cells were harvested via trypsinization, resuspended in DMEM/F12/FBS, and seeded at a density of 75,000 cells/Transwell (225,000 cells/cm^2). Primary epithelial cells were harvested via trypsinization and seeded at 50,000–75,000 cells/Transwell (150,000–225,000 cells/cm^2). Apical medium was changed 24 hr after seeding to remove non-adherent epithelial cells. On day 3 of co-culture, medium was changed to maintenance media comprising DMEM/F12 supplemented with 1% DC-FBS, 1% penicillin/streptomycin, and 2% Cell Maintenance Supplement (Cocktail B) (LifeTechnologies CM4000) on the apical side (100 μL) and Williams E Medium (LifeTechnologies A1217601) supplemented with 1% penicillin/streptomycin, 4% Cell Maintenance Supplement (Cocktail B) (LifeTechnologies CM4000) and 100 nM

hydrocortisone (Sigma 50-23-7) on the basolateral side (600 μL), with changes every 2–3 days thereafter.

2.4. Hormone-mediated decidualization of epithelial and stromal co-cultures and primary encapsulated endometrial stromal cells

Endometrial co-culture decidualization was assessed by stimulation with 0.5 mM 8-bromoadenosine 3′,5′-cyclic monophosphate (Sigma B5386) and 1 μM medroxyprogesterone 17-acetate (MPA) (Sigma M1629) in the apical and basal medium starting on days 9 and 12 of co-culture, respectively, according to common protocols previously described.[39,40] Apical medium (100 μL) was collected on days 5, 7, 9, 12, and 15 of co-culture and stored at −80 °C until analyzed by ELISA for proteins IGFBP-1 (R&D systems DY871) and prolactin (R&D systems DY682), indicative of secretory differentiation. Protocols provided by the manufacturer were adapted to allow ELISAs to be performed in a 384-well plate (ThermoFisher 464718) to minimize medium (sample) volume needed (see Supplementary Information). For primary patient endometrial stromal cell (ESCs) monocultures, cells were incubated with hormone-containing media on days 0, 3, and 6 of culture, and apical conditioned media (100 μL) samples were collected on days 3, 6 and 9 of culture. Reported values are the mean of 3–6 (apical samples) biological replicates (different gels) minus mean concentration of no-cell gel controls.

2.5. Biochemical assays

DNA synthesis assay—Click-iT EdU Alexa Fluor 488 kit (Life Technologies) was used to quantify cells actively synthesizing DNA. On days 4 or 14 of co-culture, hydrogels were incubated with 10 μM of 5-ethynyl-2′-deoxyuridine (EdU) for 4 h for tHESC and Ishikawa cultures (or on day 15 for 24 h for primary co-cultures) at 37 °C, 95% air, 5% CO_2. Cells were fixed with 4% formaldehyde in 1× PHEM buffer and MQ for 1 h at RT. Cells were washed twice with 3% BSA in PBS and permeabilized with 0.5% Triton X-100 in PBS for 20 min at RT while shaking. Click-iT reaction cocktail was prepared as described by the manufacturer and 100 μL per well was added apically and 400 μL per well added basally. Cells were incubated for 30 min at RT protected from light while shaking. After cells were washed once with 3% BSA in PBS and once with PBS, they were incubated with DAPI diluted 1:1000 in PBS for 30 min at RT protected from light. Cells were stained with anti-Cytokeratin 18 or anti-CD10 as indicated below, washed twice with PBS and imaged using a Leica DMI 6000 microscope and Oasis Surveyor software. Total number of DAPI nuclei and total number of EdU nuclei were counted using ImageJ64 software. The percentage of cells synthesizing DNA was computed as the ratio of EdU positive cells divided by the total number of DAPI counterstained cells. Reported values are the mean of at least 3 ROIs for two technical replicates per condition.

Hydroxyproline assay for collagen quantification—The hydroxyproline content, indicative of collagen content, of a Transwell hydrogel was measured using the Hydroxyproline Assay Kit (Sigma MAK008). Briefly, 2–3 gels from each culture condition were combined and hydrolyzed in 100 μL 12 M HCl at 120°C in a heat block for 3 h. Hydroxyproline standards were prepared according to the manufacturer's protocol. The hydrolyzed sample was transferred to the 96-well plate with standards and incubated at 60°C

to evaporate to dryness. The plate was allowed to come to RT after overnight incubation and 100 μL of chloramine T/oxidation Buffer was added to each well and incubated at RT for 5 min followed by incubation with 100 μL/well 4-(dimethylamino)benzaldehyde (DMAB) for 90 minutes at 60°C. Absorbance was measured using a plate reader at 560 nm. Eight-point linear standard curves were used to calculate concentrations for each sample replicate. Reported values are the mean fold change of hydroxyproline content of 4 experiments normalized to total DNA content per condition where 2–3 hydrogels were pooled per condition per experiment. Values with matrix binding peptides were normalized within each experiment to the *PHSRN-K-RGD* only condition.

Cell lysis and DNA quantification—Transwell hydrogels were prepared for lysing by rinsing twice with warm 1× PBS (100 uL apical, 600 uL basal). Apical and basal PBS were removed and 100 uL of RIPA buffer (Pierce Thermo 89900) (25 mM Tris•HCl pH 7.6, 150mM NaCl, 1% NP-40, 1% sodium deoxycholate, 0.1% SDS) supplemented with 1% phenylmethanesulfonyl fluoride (PMSF) (Sigma 93482) and 1% Protease Inhibitor Cocktail (Sigma P8340) was added apically to each Transwell hydrogel. The hydrogel was scraped with a pipet tip, then the plate was shaken on a plate shaker for 15 min at 4 °C. The lysate and gel were transferred to a tube and vortexed. Lysates were clarified by centrifugation at 16K rcf for 15 min at 4 °C. Supernatant was transferred to a new tube and frozen at −80 °C with a lysis buffer blank until further use.

The Quant-IT PicoGreen dsDNA Kit (Life Technologies P7589) was used to measure dsDNA in lysed endometrial co-cultures and used to normalize other metrics (IGFBP-1, prolactin, and hydroxyproline) to estimated cell populations. Lysates and RIPA buffer blank were diluted 20-fold in 1× TE Buffer. Samples and standards (50 μL) were incubated, protected from light, in 50 μL of detection reagent (diluted 1:200 in 1× TE buffer) for 5 min at RT. Fluorescence was measured in a plate reader at 480 nm excitation and 520 nm emission. Sample dsDNA concentration was the average of technical duplicates determined from the standard curve and multiplied by the dilution factor after subtraction of a no cell hydrogel blank.

Cytokine Luminex assay—Cytokines in 48- or 72-hour undiluted conditioned apical medium from various timepoints during the co-culture period were measured by Luminex assay using the magnetic Bio-Plex Pro Human Cytokine 27-plex assay (BioRad). Protocols provided by the manufacturer were adapted to allow the assay to be performed in a 384 well plate to avoid introducing batch effects. Ten-point standard curves plus blanks (apical medium) were included for quantification.

For each cytokine, 5-parameter logistic curves were fitted to the standards, excluding the blanks, using the L5P function in MATLAB (MathWorks)[41] Curve fits were used to calculate concentrations for each sample replicate. Median fluorescence intensities (MFI) for the samples below the lower asymptote or above the upper asymptote of the fit were imputed to be either the MFI of the minimum asymptote or 99% of the MFI of the maximum asymptote, respectively. Values reported in tables are the mean of 2 technical replicates for the Luminex assay and the number of gel replicates (n) specified in figures/tables. Concentrations that fell above the highest standard but below the maximum asymptote (due

to incomplete coverage of the quantifiable range by the standard curve) were judged to be unreliable; these values are given as greater than the concentration of the highest standard and excluded from statistical testing.

2.6. Immunofluorescence and microscopy

Samples were fixed in a 4% paraformaldehyde PHEM buffer (Electron Microscopy Sciences) for 1 h, permeabilized in 0.2% TritonX-100 in PBS (Sigma) for 30 min, and blocked for 1 h in 1% BSA (Sigma), 5% normal donkey serum (Electron Microscopy Sciences) PBS at room temperature. Hydrogels were incubated with primary antibodies (1:100, except anti-Cytokeratin 18 1:250) and rhodamine phalloidin (1:1000) (Life Technologies) overnight while rocking at 4°C, rinsed with blocking buffer 3 times (5 min each while rocking at RT), followed by secondary staining with AlexaFluor488 or AlexaFluor568-conjugated donkey anti-rabbit and anti-mouse IgG (1:500) (Invitrogen) overnight while rocking at 4°C. Cell nuclei were counterstained with DAPI (1:1000) (Life Technologies) for 15 min at RT. Finally, hydrogels were rinsed 3 times with 1× PBS (5 min each) and rocked overnight prior to mounting using Prolong Gold Antifade (Life Technologies P36935) on glass coverslips. Primary mouse antibodies included RPE conjugated anti-CD10 (Dako, SS2/36) anti-Fibronectin (EMD Millipore FBN11, Ab-3, Calbiochem CP70), anti-Collagen I (EMD Millipore MAB3391), and primary rabbit antibodies included anti-Collagen IV (Abcam ab6586), and anti-Cytokeratin 18 (Abcam ab52948).

Phase images were acquired using a Leica DMI 6000 microscope and Oasis Surveyor software for unfixed hydrogels *in situ* in culture inserts. Confocal images were acquired using a Nikon Spinning Disk Confocal Microscope or the Nikon A1R Ultrafast Spectral Scanning Confocal Microscope and Nikon NIS Elements acquisition software on fixed and coverslip-mounted hydrogels. Fibrillar collagen was detected by second harmonic generation microscopy using an Olympus FV1000 Multiphoton Laser Scanning Confocal Microscope and Olympus acquisition software on unfixed hydrated hydrogels, gently cut away from culture inserts and placed carefully on coverslips. Second harmonic channel was background-corrected by subtraction of the autofluorescence signal collected at 488 nm.

2.7. Statistical analysis

Data are expressed as average ± standard error of the mean (SEM). Statistical analysis was performed using GraphPad Prism v.5 for Mac OS X. Unpaired t-tests assuming unequal variances and two-way ANOVAs with appropriate post-tests were performed as indicated in the results. Statistical significance was defined as * $p < 0.05$, ** $p < 0.01$, *** $p < 0.0001$.

3. Results and Discussion

A 2-D attachment screen identifies PHSRN-K-RGD as a suitable ligand for initial attachment of both epithelial and stromal cells

Epithelial and stromal cell phenotypes *in vitro* are sensitive to both the biochemical and biophysical properties of integrin ligands that mediate cell attachment.[42–47] In order to identify peptides that foster the greatest degree of cell-matrix interactions in the initial stages

of culture, we assessed attachment of stromal and epithelial cells to the surface of peptide-modified polyethylene glycol (PEG) hydrogels. Epithelial cells or stromal cells were seeded in serum-containing medium onto the surfaces of hydrogels synthesized by crosslinking 8-arm peptide-functionalized PEG macromers, fPEG-VS, with a dithiol MMP-sensitive peptide crosslinker, *MMP-CL*, as shown schematically in Figure 1A. A panel of four peptide sequences derived from ECM proteins found in the endometrium and offering a range of published integrin specificities (see Methods for full sequences), was tested: fibronectin(FN)-derived *RGD*, recognized by $\alpha_v\beta_3$ and weakly by other integrins; a synthetic branched peptide, *PHSRN-K-RGD*, mimicking the FN-III 9–10 domain binding sites recognized by integrins $\alpha_5\beta_1$ and $\alpha_3\beta_1$;[29,43,44] a collagen I-derived peptide, *GFOGER*, reported to engage integrin $\alpha_2\beta_1$ and others;[30,48] and *Lam-5* a peptide derived from the basement membrane protein laminin 5 that reportedly engages integrin $\alpha_3\beta_1$.[31] Each peptide was included at various nominal concentrations (0, 0.25, 0.5, and 1.0 mM) during crosslinking, resulting in actual final concentrations in the hydrogel of about half these initial values (0, 0.12, 0.23, and 0.47 mM) after post-crosslink equilibrium swelling.

As expected, after 6 hours of attachment, neither stromal nor epithelial cells showed significant attachment to gels lacking adhesion peptides (Fig. 1B). The FN-derived peptides *RGD* and *PHSRN-K-RGD* conferred a statistically significant attachment advantage over *GFOGER* and *Lam-5* peptides at all concentrations tested for tHESCs, and at the highest nominal peptide concentration, *PHSRN-K-RGD* enhanced attachment of tHESCs significantly compared to all other peptides. *PHSRN-K-RGD* showed enhanced attachment for Ishikawa epithelial cells at nominal concentrations of 0.5 and 1 mM, and we have previously found that *PHSRN-K-RGD* also provides an adequate adhesion environment for attachment of primary endometrial epithelial cells to 2D PEG hydrogels.[23]

Identification of the fibronectin-derived peptide sequence, *PHSRN-K-RGD*, as suitable for endometrial cell attachment is conceivable as the endometrial stroma contains fibronectin during all stages of the menstrual cycle and increases in expression in response to progesterone-mediated differentiation during the days prior to menstruation.[49,50] The dynamics of fibronectin expression in the endometrium correspond with dynamic endometrial epithelial and stromal cell expression of fibronectin-binding integrins,[50,51] and a lack of endometrial fibronectin following ovulation has been observed in infertile women.[52] Hence, we selected *PHSRN-K-RGD* as the primary attachment peptide for further studies, as it supports both stromal and epithelial matrix engagement in the early stages of culture.

Primary human endometrial stromal cells encapsulated in peptide-modified PEG gels exhibit functional viability

Following identification of a fibronectin-derived peptide, *PHSRN-K-RGD*, that supports initial attachment of both endometrial epithelial and stromal cells to a synthetic PEG hydrogel ECM, we next evaluated the functional hormone-responsive phenotypic behavior of primary human endometrial stromal cells when encapsulated within 3D hydrogels. Specifically, hydrogels (comprising 5 wt% fPEG-VS and 40% crosslinked) contained the attachment peptide *PHSRN-K-RGD* (0.5 mM nominal concentration) and two additional peptides intended to capture local cell-secreted ECM. Matrix-binding peptides were

designed to capture fibronectin (*FN-binder*, 0.25 mM) produced by endometrial stromal fibroblasts throughout the cycle[49,52] and both laminin and type IV collagen basement membrane proteins (*BM-binder*, 0.25 mM) that are normally produced by the epithelium during all menstrual cycle stages and locally produced and accumulated in the pericellular region of hormonally responsive fibroblasts in the stroma.[49,52,53]

Primary patient endometrial stromal cells (ESCs) from three different donors in the proliferative phase of the menstrual cycle were encapsulated within PEG hydrogels and assessed for the ability to undergo functional secretory differentiation (decidualization) in response to hormonal cues 0.5 mM cAMP and 1 μM medroxyprogesterone acetate (MPA) as described previously.[39,40] These decidualization cues were added at the start of the culture and in each medium replacement (see Methods). At day 9 following initiation of culture, ESCs in control cultures (no stimulation) showed elongated and spindle-shaped morphologies while ESCs stimulated with decidualization cues showed plump, rounded morphologies characteristic of a decidualization phenotype (Fig. 2A). While cytoplasmic shape changes were observed by phase contrast imaging, no difference in nuclear shape was found between control and cAMP/MPA stimulated primary cells (Supplementary Fig. S1) as has been previously described for an endometrial stromal cell line cultured in 3D collagen gels under decidualization conditions.[15] Secreted proteins IGFBP-1 and prolactin increased in stimulated conditions on days 3, 6 and 9 (after being stimulated on days 0, 3, and 6) of culture as compared to unstimulated ESCs, which did not secrete decidual proteins above the assay detection limits (Fig. 2B). Primary stromal cells were both viable and capable of hormone-mediated differentiation when encapsulated within the PEG hydrogels, suggesting that these cells would be capable of dynamic hormonal paracrine interactions when co-cultured with endometrial epithelial cells.

Epithelial monolayer morphology and stromal cell remodeling are influenced by crosslink density in long-term epithelial-stromal co-cultures

After establishing that primary endometrial stromal cells maintained a hormone responsive phenotype when encapsulated in 3D hydrogels, we explored the phenotypic effects of varying hydrogel crosslinking density on the establishment and evolution of relevant co-culture characteristics using cell lines as an initial model system. Co-culture features over the first two weeks, including epithelial barrier formation and encapsulated stromal cell remodeling, were investigated. For a given macromer composition and weight percent, synthetic ECM mechanical properties (including bulk stiffness and nano-scale ligand biophysical presentation), permeability, and topology are governed by the extent of crosslinking. The extent of crosslinking also governs the ease with which cells can remodel the synthetic ECM as the crosslinker can be cleaved by cell-associated proteinases. Hence, we varied crosslink density as the independent variable, recognizing the resulting epithelial monolayer and encapsulated stromal cell behaviors represent a convolution of responses to the properties affected by the crosslink density.

We formed gels by first reacting 8-arm PEG-VS macromers with adhesion and matrix binding peptides with a stoichiometry to yield an average of 0.7 peptides/PEG macromer (10% modification, 2:1:1 *PHSRN-K-RGD:FN-binder:BM-binder*, nominal 1 mM total).

PEG macromers were combined with various concentrations of dithiol peptide crosslinker resulting in 40–70% of total macromer arms crosslinked. The hydrogels were crosslinked with *MMP-CL* peptide, containing the substrate GPQGIAGQ, which is reportedly cleaved by MMP2 and MMP9, allowing remodeling by cellular proteinases.[21,54,55] We selected a substrate with intermediate cleavage kinetics from among those reported in the literature,[21] aiming to achieve gradual remodeling and replacement by cell-produced ECM over two weeks in culture. The actual post-swelling total peptide concentration (excluding crosslinker) ranged from 0.5 mM (40% crosslinking resulted in 2.2 swollen/initial volume) to 0.7 mM (70% crosslinking resulted in 1.5 swollen/initial volume).

Epithelial monolayer formation on top of the hydrogel was investigated as chemical, mechanical, and topological features of the underlying substrate are known to influence the initiation and progression of an epithelial monolayer.[56–58] The gel formation, including stromal cell encapsulation, was carried out during a centrifugation step to eliminate the meniscus, as we found that gel curvature compromised the epithelial barrier integrity, resulting in patchy areas near the edges of high curvature as has been reported for other epithelia.[56,59] These denuded areas were not observed on flat gels or on gel-free culture inserts (Fig. 3A). All gel crosslinker conditions resulted in a confluent epithelial layer by day 4 after initially seeding 7.5×10^4 Ishikawa cells (Fig. 3B). However, by day 12, defects (holes) were observed in epithelial layers cultured on the most highly crosslinked gels, and complete delamination was observed at 70% crosslinking. Few defects developed in the epithelial monolayer of gels for the 40% crosslinker condition, even after two weeks in co-culture.

Next, we evaluated the ability of encapsulated stromal fibroblasts to elongate and migrate within the hydrogel over two weeks in co-culture. Stromal fibroblasts, which were displaced to regions of the gel near the membrane during initial gel formation and centrifugation, remained rounded at days 7 and 14 in the 70% crosslink condition, unless they were in direct contact with the membrane (Fig. 3C). In contrast, stromal fibroblasts encapsulated in the 40% crosslinked gels and co-cultured with an Ishikawa epithelial monolayer appeared to migrate toward the epithelial layer from their initial position close to the membrane, as they were present in the middle of the gel at days 7 and 14 and showed enhanced elongation near the epithelial layer (Fig. 3C). The epithelial layer produces cytokines that may stimulate such migration, including PDGF-BB (Supplementary Table S2).[60,61] One explanation for the failure of cells to elongate and migrate in the 70% crosslink condition is that the cells must cleave a greater number of crosslinks, and are kinetically trapped, but an additional plausible explanation is that the dense crosslinks also obscure access to the adhesion ligands, and may prevent the integrin clustering required to gain sufficient signaling and traction for motility.[62–64]

Additional insight into the evolution of the encapsulated stromal cell behavior is revealed by examination of the thickness of the stromal layer, as the thickness represents a balance of both gel swelling due to crosslink cleavage and gel contraction due to cells depositing new matrix. Phase images of the epithelial layer and the culture insert membrane were used as boundaries to measure the in situ gel height. Measurements were the average of three locations across the diameter of the hydrogel over three weeks in cultures. Scans in the focal

plane of the epithelial layer of each culture showed variation of (~30 um in height) evolving after the first week, due to formation of dome-like structures in the epithelium that spanned ~100 um in width. Hydrogels heights of ~450 μm and ~475 μm were consistently observed for the 70% and 40% crosslinked gels, respectively (data not shown). Stromal cells encapsulated in collagen gels often shrink substantially in dimension during culture due to matrix compaction,[16,22,65] whereas synthetic gels typically swell upon cleavage of crosslinks.[66] Even though the encapsulated cell concentration (nominally 4×10^6 cells/cm^3) was at least twice the value commonly reported for encapsulated stromal cultures,[16,65,67] gels did not change dimensions significantly. We therefore examined additional phenotypic behaviors, including matrix accumulation, using the 40% crosslink condition as it permitted epithelial barrier formation and fibroblast proteolytic remodeling and migration to occur.

Matrix-binding peptides enhance accumulation of cell-secreted ECM by Ishikawa epithelial cells

The initial establishment and subsequent evolution of cell-matrix interactions may be influenced by different peptides within the synthetic ECM. After identifying peptides that mediate initial cell attachment, *PHSRN-K-RGD*, and crosslinker conditions that allow cell protease remodeling of the microenvironment, we investigated how inclusion of peptides with affinity to matrix proteins influences deposition and organization of local cell-produced ECM. Cell-secreted ECM anchors cells to their microenvironments and regulates myriad cell functions from survival to differentiation.[68–70] The basement membrane, a specialized ECM enriched in laminin, type IV collagen, and various heparan sulfate proteoglycans, underlies the epithelial layer and separates epithelial and stromal compartments.[69] Although epithelial cells produce basement membrane proteins at their basolateral surfaces in culture, PEG gels tend to resist protein adsorption, and thus ECM produced by cells may disperse into the culture medium and fail to accumulate to significant levels. We speculated that inclusion of small peptides that bind to ECM proteins might foster more robust ECM deposition in a locally responsive manner – i.e., accumulation of basement membrane proteins by epithelial cells and a stromal matrix (fibronectin evolving to fibrillar collagen) by stromal cells.

To test the effects of *FN-binder* (fibronectin) and *BM-binder* (collagen IV and laminin) on ECM accumulation, we reconsidered the constraint on total peptide concentration in light of the results from Fig. 3, which show that the 40% crosslinking condition is preferable for morphogenesis of stroma and stable retention of the epithelial layer in co-cultures of endometrial cell lines. The total combined concentration of functional peptides (i.e., *PHSRN-K-RGD*, *FN-binder*, and *BM-binder*) in the gel is constrained by the common VS-thiol chemistry used for both crosslinking and functionalization. Near-complete reaction of the 8 pendant VS-groups on the PEG macromers is required to achieve 70% crosslinking for a total nominal functional peptide concentration of 1 mM, which affords only 0.5 mM *PHSRN-K-RGD* integrin-binding peptide, a concentration below the 1 mM associated with enhanced attachment of stromal cells in the 2D studies (Fig. 1B). We therefore chose a nominal 2 mM total peptide concentration (1 mM *PHSRN-K-RGD*, 0.5 mM *FN-binder*, 0.5 mM *BM-binder*) to further enhance interactions with stromal cells for future studies involving longer-term cultures and more detailed investigations of phenotypes. Indeed, this

gel formulation resulted in culture morphologies characterized by fewer and smaller defects in the epithelial layer over more than two weeks, and redistribution of a significant fraction of the stromal cells from the near-membrane region up into the gel near the epithelial cells (Fig. 4A).

Having verified that the 2 mM total peptide concentration resulted in enhanced morphological phenotypes, we then examined whether *BM-binder* influenced ECM accumulation and other properties of the epithelial layer by immunostaining constructs at the one week time point after a confluent monolayer was achieved. Epithelial cells (Ishikawa) attached, proliferated, and formed an epithelial sheet when seeded at 2.3×10^5 cells/cm^2 in all conditions with or without matrix binders as evidenced by immunostaining for CK-18, which anchors hemidesmosomes and actin structures to the underlying basement membrane (Supplementary Fig. S2). However, in the absence of *BM-binder* (i.e., in gels containing no matrix binders, or just *FN-binder*), accumulation of basement membrane (as assessed by collagen IV immunostaining) by the epithelial layer after one week of co-culture was very sparse, even in the presence of *FN-binder* (Fig. 4B). This is consistent with known properties of basement membrane assembly, which proceeds independent of fibronectin.[71,72] In contrast, abundant collagen IV immunostaining was observed beneath epithelial cells when *BM-binder* was included in the gels used for co-culture (Fig. 4B). Furthermore, collagen IV matrix patterning appears similar to cytoskeletal protein CK-18 organization suggesting that matrix binders may also contribute to the structural organization of the epithelial layer rather than simple accumulation of basement membrane matrix.

The images in Fig. 4B represent a shallow composite z-stack (30 μm) as the surface of the epithelial layer undergoes morphogenesis in the first week to create small domes and valleys; hence, the composite image includes some regions of closely-associated fibroblasts, which also stain positive for pericellular collagen IV. Individual z-planes of the Fig. 4B projection image illustrate that there is abundant collagen IV staining associated with long thin fibroblasts (Supplementary Fig. S3, arrows) that have migrated and are closely associated with the epithelial layer in all of the tested conditions. Fibroblasts were visualized in the same plane as Ishikawa nuclei in many instances.

Migration and intimate association of stromal fibroblasts with epithelia is consistent with other heterotypic cell culture systems where pericellular fibroblasts may become locally activated contributing to matrix production of collagens and fibronectin immediately surrounding adjacent epithelia.[73,74] The presence of collagen IV in the stromal layer is expected as endometrial fibroblasts, like fibroblasts from many other tissues, produce collagen IV.[53] However, collagen IV immunostaining in the stromal layer was strongly visible only in the upper region of the co-culture, near the epithelial cells, and was faint in the deeper regions of the stroma (data not shown), suggesting that collagen IV in the pericellular region of the fibroblasts may derive primarily from interactions with epithelia. In normal human endometrium, collagen IV immunostaining is localized to the basement membrane except during hormone differentiation where decidual cells (stromal fibroblasts that undergo differentiation in response to hormones) secrete basement membrane proteins locally around themselves, including collagen IV and laminin.[49,52,75,76] Since we used the tumor-derived Ishikawa epithelial cells and the human immortalized stromal cells, the

appearance of collagen IV staining in the stromal layer near the epithelia may arise from the transformed nature of these cells, or it may reflect that the early stages of culture are similar to a wound-healing phase where provisional matrix is deposited as a transition to regenerated normal tissue structure.[77] Our goal in these screening studies was to determine if the matrix-binding peptides could locally influence matrix accumulation, and indeed, enhanced collagen IV accumulation and organization was observed when the matrix-binding peptide, *BM-binder*, was present.

Matrix-binding peptides enhance accumulation of cell-secreted ECM by stromal cells

Having established that *BM-binder* and *FN-binder* peptides in combination dramatically enhanced accumulation of collagen IV at the basal surface of the epithelial layer, we investigated the influence of these peptides on the accumulation and properties of ECM secreted by stromal cells encapsulated in the gel beneath the epithelial layer. Both cell-produced and plasma-derived fibronectin are major components of provisional stromal wound-healing matrices that are ultimately remodeled to collagen-rich ECM that replaces the fibronectin-rich scaffold.[77] Fibronectin binds collagens and other ECM molecules to facilitate this evolution of ECM architecture.[72] We included *FN-binder* in the gel to facilitate the natural stromal ECM evolutionary process, speculating that stabilization of FN secreted by stromal cells immediately after encapsulation would provide a foundational ECM for further matrix deposition and remodeling.

Fibronectin accumulated in all conditions after two weeks with no discernible differences at the level of immunostaining (Supplementary Fig. S4), which is not surprising as the gel encapsulating the stromal cells likely hinders diffusion of fibronectin away from the pericellular region and immunostaining does not reveal subtle differences in ECM organization, or presence of other cell-produced ECM molecules that might bind to FN to create a more fully assembled ECM. In order to further probe ECM composition and structure, we live-imaged the stromal layer with two-photon second harmonic imaging to visualize fibrillar collagens (i.e., collagens I-III and others, excluding the non-fibrillar collagen IV).[78,79] A cell associated second harmonic signal was observed in the presence of matrix binding peptides, especially the *FN-binder*, but was absent without matrix stabilizing peptides (Supplementary Fig. S5). The signal was greatly enhanced when both matrix binders were present, indicative of organized structural matrix assembly.

Further quantification of collagen matrix proteins was assessed by measurement of hydroxyproline, an analog of the amino acid proline that is post-translationally hydroxylated, and is found in abundance in collagen matrix proteins. Collagen content was increased in all conditions with matrix binders present, and was greatest in the condition with both *FN* and *BM-binder* likely due to enhanced stabilization of various collagens, including both fibrillar collagens and collagen type IV (Fig. 4C). In particular, a 1.3-, 1.1- and 1.5-fold increase in hydroxyproline content (when normalized to total DNA per condition) was associated with the presence of *BM-binder* alone, *FN-binder* alone, or *BM-binder* + *FN-binder*, respectively when compared to *PHSRN-K-RGD* alone. *BM-binder* resulted in statistically significant increases in hydrogel hydroxyproline content, which is likely due in part to the stabilization of collagen IV basement membrane matrix at the

hydrogel epithelial barrier interface. These differences in matrix deposition were observed in conditions that are likely less than optimal overall for matrix deposition, as cells were maintained in a standard culture medium containing 0.01 mM ascorbate in the basal compartment, rather than in conditions that boost collagen production by supplementing with additional ascorbate to compensate for oxidation and depletion.[80,81] Further, softer matrices are less conducive to accumulation of fibrillar collagen compared to stiffer environments.[82] Fine tuning these environmental parameters, along with carrying out studies with primary cells, may reveal further differences in how the combination of matrix-binding peptides influences evolution of cell-secreted ECM.

In vitro endometrial cell line co-cultures are proliferative and hormone responsive for at least 2 weeks

Having established a synthetic ECM composition that fosters desirable morphologies and matrix accumulation, we then examined the proliferative and hormone responsive phenotypes of these cultures. The cultures were maintained in low serum conditions starting on day 3 (1% FBS in apical medium; 0% serum in basal medium); nevertheless, Ishikawa epithelial cells exhibited robust and sustained proliferation throughout the culture period (34.7 ± 2.5% and 34.5 ± 1.9% of nuclei stained positive for EdU after 4-hour incorporation on days 7 and 14, respectively; Fig 5A). This proliferation of Ishikawa cells in low serum is consistent with other reports.[83,84] Stromal cells (tHESCs) encapsulated in the 3D synthetic ECM similarly showed sustained, though less pronounced, proliferation (18.9 ± 4.0% and 19.3 ± 1.9% of cells incorporated EdU over 4 hours on days 7 and 14, respectively), with proliferative cells distributed throughout all regions of the hydrogel (Fig. 5A). This stromal proliferation rate is consistent with observations of ~3-fold increase in DNA content when dermal fibroblasts were encapsulated in RGD-modified PEG gels and cultured for two weeks.[22]

We initially seeded 1.25×10^5 total cells (7.5×10^4 Ishikawa and 5×10^4 tHESC), corresponding to ~ 1 μg of total DNA. The increase to ~2 μg of total DNA present at days 12 and 24 of co-culture represents roughly one population doubling of the cells that were initially seeded. Interestingly, despite the observed sustained DNA synthesis, the total DNA content of the cultures (i.e., combined epithelial and stromal cells) showed insignificant change from day 12 to day 24 (Supplementary Fig. S6), suggesting cells are being lost from the cultures at the same rate as they are being produced.

The most likely mechanism of cell loss is through continuous dynamic morphogenesis of the epithelial layer involving groups of cells that form domes and then detach either by terminal differentiation and apoptosis or by budding off as clumps that float in the apical medium, leaving a defect in the monolayer. Epithelial barriers are known to undergo dynamic growth, differentiation and morphogenic processes to replace terminally differentiated cells which are thought to comprise locally formed domes.[11,84,85] Domes and valleys in the epithelial monolayer were observed after the cells reached confluence (around one week of co-culture), and these morphological features persisted during the remaining culture weeks. Visualization of both intact domes (arrows) and a subsequent barrier defect are representative of features observed after three weeks in co-culture (Fig. 4A, day 25 of co-

culture). The domes appear to be the result of epithelia detaching from the hydrogel surface and extending into the apical media as evidenced by the lack of nuclei in contact with the hydrogel surface underneath these raised structures. Additionally, we observed that over the course of a couple days, some dome regions collapsed resulting in holes or defects in the monolayer with visible cell debris present within. This is consistent with cell death in response to loss of cell-matrix interactions. We observed that domes were more likely to remain intact, without progression to a barrier defect, in conditions with less crosslinking (40% versus 70%) or higher adhesion ligand density (2 mM versus 1 mM total nominal peptide), possibly suggesting that ligand accessibility and integrin clustering ability may be important for maintenance of epithelial layer integrity.

Finally, the cultures remained hormone-responsive, as assessed by the response to decidualization cues 0.5 mM 8-Br-cAMP and 1 μM medroxyprogesterone acetate (MPA). When these were added on days 9 and 12, they elicited significant increases in secretion of IGFBP-1 and prolactin measured on days 12 and 15 (Fig. 5B). The decidualization response is marked by secretory protein production of IGFBP-1 and prolactin by endometrial stromal cells in response to decidualizing cues including progestogens (MPA, progesterone) and cAMP.[15,40,86] As previously reported for other culture configurations, where co-stimulation with cAMP sensitized stromal cells to MPA induced decidual protein production,[40] no stimulation by estradiol was required prior to addition of decidualization cues in order to elicit production of decidual proteins prolactin and IGFBP-1 in this 3D in vitro model system. The establishment of this long-term co-culture system may enable future studies of how endometrial phenotype is regulated throughout an entire menstrual hormonal cycle, comparing primary cells from healthy and diseased patients, for example. After establishing that synthetic matrix hydrogels supported viable and hormonally responsive cell line co-cultures, we investigated intercellular cytokine communication for cell line and primary co-cultures.

Apical cytokine and growth factor environment of co-cultures is conditioned primarily by epithelial cells

The immune and growth factor signaling milieu is important for cyclic remodeling of the endometrium and has been implicated in numerous endometrial pathologies.[87,88] We therefore evaluated production of 27 cytokines, chemokines, and growth factors using a multiplex immunoassay of apical cell culture supernates in cell-line co-cultures in order to establish protocols and a baseline for subsequent comparison to primary cells. First, we assessed the cytokine environment, as measured by 48 hour conditioned medium collected on days 7 and 15 of coculture, to establish how much the signaling milieu varies during the culture period (Fig. 6A). We found that most cytokines changed less than 2-fold (dashed lines), with most exceptions also having high replicate variability (PDGF-BB, VEGF, Eotaxin). The only cytokine which was consistently increased on day 15 vs. day 7 was MCP-1, which is secreted primarily by the stromal cells, and may require time to diffuse through the gel and pass through the epithelial barrier before accumulating in the apical medium.

We next examined the contributions of stromal (tHESC) and epithelial (Ishikawa) monocultures to apical cytokine measurements, compared to co-cultures of these cells, at day 15 (Fig. 6B and Supplementary Table S2). Among the 27 cytokines measured for cell lines on day 15, eight cytokines (TNF-α, RANTES, MIP-1α, IL-5, IL-1β, G-CSF, and FGF basic) were below the limit of detection for both single cell lines, although one (MIP-1α) was detectable, albeit at very low levels, in co-culture. Another 11 cytokines (VEGF, PDGF-BB, MIP-1β, IL-9, IL-7, IL-4, IL-17A, IL-13, IL-12p70, IL-10, and GM-CSF) were below the detection limit in stromal cultures alone, but produced abundantly and at similar levels in Ishikawa alone and co-cultures, suggesting that these are produced exclusively by Ishikawa epithelial cells in a stromal-independent manner. Three cytokines (IL-15, MCP-1, and Eotaxin) were secreted at higher levels by tHESCs than by Ishikawa cells. One of these, MCP-1, was produced abundantly by stromal cells but was almost undetectable in Ishikawa monoculture, and present in co-culture at greatly reduced (15%) levels compared to stromal mono-culture, suggesting this cytokine is produced by stroma and its access to the apical compartment may be restricted by the epithelial barrier. IL-8, IL-6, and IL-2 were produced at slightly higher levels by epithelial cells than stromal cells in monoculture, with little effect of co-culture. IP-10, IL-1ra, and IFNγ were produced at dramatically higher levels by epithelial cells than stromal cells.

Primary 3D endometrial stromal and epithelial co-cultures are proliferative and respond to decidualization cues

While cell line models may provide reproducibility and some tissue specific function for some applications, primary cells offer the ability to elucidate differences in cytokine and growth factor cell-cell communication networks that may arise from normal biological heterogeneity in healthy women, and are needed to construct models of disease mechanisms in sample from diseased patients. We therefore evaluated the ability of the synthetic matrix (1 mM *PHSRN-K-RGD*, 0.5 mM *BM-binder*, and 0.5 mM *FN-binder* nominal with 40% crosslinking) to support proliferation and hormone responsiveness of primary endometrial cells (isolated from proliferative biopsies) over two weeks in co-culture.

Since a single standard biopsy typically yields only 0.2–2 × 10^6 primary epithelial cells from proliferative phase endometrium, we investigated a range of seeding densities based on a benchmark of 10^5 cells/insert (3 × 10^5 cells/cm^2) for forming a monolayer of epithelium on transwells.[11] Cells were maintained for at most one week in culture prior to establishment of between 4–12 co-cultures per donor (see Methods). Epithelial monolayers formed for one donor (Fig. 7A) when epithelial cells were seeded at 7.5 × 10^4 cells per culture insert (2.3 × 10^5 cells/cm^2) resulting in 430 μm^2 per cell, or 21 μm center-to center spacing. Lower seeding densities were ineffective: epithelial cells from two additional donors, seeded at 5 × 10^4 cells/insert (1.5 × 10^5 cells/cm^2), resulted in initial incomplete coverage of the hydrogel surface and a patchy appearance throughout the entire two week culture period (Supplementary Fig. S7), despite some evidence of proliferation (see below).

Three different donor co-cultures were assessed for the ability to respond to decidualization cues. The primary donor with epithelial cells seeded at 7.5 × 10^4 cells per insert and co-cultured for two weeks with stromal cells showed dramatic morphological responses to

decidualization cues added at days 9 and 12 (Fig. 7A). CK18 and actin staining were both diffusely-localized in the absence of cAMP and MPA, but revealed a classic epithelioid layer morphology in the presence of hormones, with actin ringing the perimeter of cells (Fig. 7A). Although both conditions appear to have a contiguous cell layer revealed by actin staining, the CK18 staining in these images was not uniformly contiguous across the surface in the same regions, even when the actin stain was associated with an epithelioid morphology (Fig. 7A). Confirmation of the nature of the cells that appear to be CK18- in these images would require additional staining to rule out decidual cells (differentiated stromal fibroblasts). Concomitant with morphological changes, decidualization cues added on days 9 and 12 of culture resulted in significant increases in prolactin and IGFBP-1 protein levels on days 12 and 15 of culture (Fig. 7B). These studies establish the potential of this culture system to respond to physiological cues, and provide a foundation for future investigations of a broader range of physiological stimuli and responses involved in dynamic behavior of the endometrium.[89]

Additionally, DNA synthesis was assessed for two subsequent donors on day 15 of co-culture resulting in 7.8 ± 3.2% and 8.3 ± 1.6% EdU positive epithelial cells (CK18+) and 10.3 ± 3.1% and 15.5 ± 1.6% EdU positive stromal cells (CK18-) after EdU incorporation for 24 hour. Results are the average of a hormone stimulated and a control co-culture for each donor (Fig. 7C). Greater than 60% of CK18- cells were found encapsulated within the hydrogel (as opposed to spread on the culture insert membrane) after 15 days for both donors. Of those CK18- cells present on the membrane, 4.9 ± 0.3% and 5.6 ± 3.2% were EdU positive, indicating that most of the CK18- cells that were EdU positive were encapsulated within the hydrogel.

In vitro primary endometrial stromal and epithelial co-cultures produce cytokines and growth factors more abundantly than do cell lines, and in a hormonally responsive fashion

Applications of endometrial models include studies of embryo implantation, microbiome dysregulation, and effects of inflammation and exposure to environmental chemicals on endometrial function – applications where complex cell-cell communication networks regulate tissue response. Hence, we investigated the cytokine and growth factor production by primary endometrial stromal and epithelial cells from 3 different donors compared to each other and to cell lines after 1 week of co-culture (Fig. 8A and Supplementary Table S3; cytokines are ordered by median fold change of each primary cell culture over the cell lines). Overall, the primary co-cultures appeared more similar to one another than to the cell lines and had a higher level of most secreted factors compared to the Ishikawa and tHESCs. Twenty of 27 cytokines were increased in primary cells compared to the tHESC and Ishikawa cell lines. Six cytokines were not detectable in cell line co-cultures, but were detectable in at least some of the primary cell co-cultures (GM-CSF, IL-1β, IL-1ra, FGF basic, IL-2, and IL-5). Only 4 showed a decrease (IL-13, IL-12p70, VEGF, and PDGF-BB) and 3 similar levels (IL-7, IL-10, and IL-9).

These differentially-produced cytokines play diverse roles in the essential functions of the endometrium, from regulating immunity of the maternal-fetal interface at the time of implantation and beyond, to governing breakdown of tissue during menstruation. As one

example, VEGF and IP-10, which are expressed at opposite patterns in cell line versus primary co-cultures (VEGF is lower, and IP-10 much higher, in primary cells) play opposing roles in angiogenesis, with VEGF inducing and IP-10 opposing.[90] Cultured in the same microenvironment, cell lines exhibit a cytokine signature of a rapidly growing tissue fostering angiogenesis while the primary cells exhibit a phenotype of a more mature tissue. Our findings are consistent with previous reports of abundant production of VEGF by Ishikawa cells cultured in a 3D collagen-GAG matrix.[91] We also compared our measurements to previously published values for 14 of the same cytokines secreted by co-cultures of primary endometrial stromal and epithelial and, despite different time points and culture protocols, found similar trends in relative cytokine levels.[9] Possibly due to the shorter time point or media dilution effects in Chen et al., several cytokines detectable in our samples were not detected there (RANTES, IFNγ, IL-1β, IL-2, IL-5, and IL-10), but of the cytokines detectable in both studies, values reported by Chen et al. varied between 1% (TNFα) and 60% (MIP-1α) of those found here, with a median of 17%. Given the different cell culture times, cell numbers, and volume of apical medium, and assuming a constant secretion rate per cell, we would expect the values observed in Chen et al., to be about 20% of those we observed.

Finally, we examined how cytokine and growth factor production was influenced by decidualization cues in primary cells from 3 different donors. Among the 27 factors assayed, IL-15 and IL-10 levels were most prominently enhanced in all three proliferative phase co-cultures in response to decidualization cues (Fig. 8B and Supplementary Table S4; statistically significant in one donor). An increase in endometrial IL-15 mRNA during the secretory phase has been observed *in vivo*, indicating that this model system is able to reproduce aspects of *in vivo* cytokine behavior in response to hormones.[92] In addition, progesterone has been demonstrated to modulate IL-10 response to LPS-stimulation, as a model of infection[93] and low levels of endometrial IL-10 are observed in women with recurrent spontaneous abortion.[94] Interestingly, in our data, levels of baseline IL-10 varied widely across subjects, suggesting that the ability to follow cells from the same subject over time is critical to understanding hormone-responsive cytokine behavior. Additional cytokines (Eotaxin and MIP-1β) showed donor-specific variability in response to hormone treatment (Supplementary Table S4). Here, we demonstrate the ability to elucidate intercellular cytokine signaling in response to decidualization cues and donor specific variation in immune signaling *in vitro* using a fully synthetic extracellular matrix to establish long-term primary cell co-cultures.

4. Conclusion

Creation of 3D barrier epithelial tissue mimics from donor epithelial and stromal cells requires a ‘one-size-fits-all’ extracellular matrix that allows for stromal cell remodeling and epithelial polarization, is permissive to matrix deposition and assembly, and fosters characteristic tissue phenotypic responses to external perturbations. Here, using the endometrium as an example mucosal barrier tissue, we define a modular synthetic ECM based on readily-available PEG macromers and synthetic peptides that fosters physiologically responsive co-cultures of epithelial and stromal fibroblast cells for two weeks in culture. The essential design features of this modular synthetic ECM include an

adhesion peptide that engages both stromal and epithelial cells, peptides that bind to and stabilize the ECM produced by each cell type in a locally-responsive fashion, and a crosslinker that is susceptible to cell-mediated cleavage to enable remodeling and evolution of tissue structure. Using this synthetic ECM, we illustrated profound phenotypic differences in co-cultures constructed from standard endometrial cell lines compared to co-cultures constructed from patient-derived primary endometrial cells with respect to production of cytokines and growth factors that regulate tissue growth, maturation, and function. The ability to generate primary endometrial cultures, utilizing cells from biopsies, facilitates further research aimed at development of patient-specific endometrial treatments with potential applications ranging from studying therapeutic drug efficacy to regenerative medicine and cell delivery strategies for treatment of Asherman's syndrome. The modular nature of the synthetic ECM, its ease of fabrication, and the delineation of design principles involved in implementing its use for new applications, together provide a foundation for its adaption for widespread application in mucosal barrier tissue engineering.

Supplementary Material

Refer to Web version on PubMed Central for supplementary material.

Acknowledgments

The authors would like to acknowledge the patients that agreed to participate through Newton-Wellesley Hospital and the study and surgical staff, including Dr. Stephanie Morris, Johanna Renggli-Frey, Emily Prentice and for technical support from Martina de Geus at MIT. We thank the Koch Institute Swanson Biotechnology Center for technical support, specifically Eliza Vasile and Jeffrey Wyckoff in the microscopy core facilities. We are grateful to Kevin Osteen for advice on endometrial biology and isolation, culture, and phenotypic evaluation of endometrial cells, and to Kaylon B. Tran and Annelien Zweemer for critical reading of the manuscript.

This work was supported in part by the John and Karinne Begg Fund supporting the MIT Center for Gynepathology Research, NIH T32 GM 008334 (Interdepartmental Biotechnology Training Program), DARPA Microphysiological Systems: Program W911NF-12-2-0039, the Manton Foundation, the NSF STC Emergent Behaviors of Integrated Cellular Systems, NIH grant DP3-DK097681 and ARO Institute for Collaborative Biotechnologies grant W91NF-09-001, and the Koch Institute Support (core) Grant P30-CA14051 from the National Cancer Institute.

References

1. Kim HJ, Li H, Collins JJ, Ingber DE. Contributions of microbiome and mechanical deformation to intestinal bacterial overgrowth and inflammation in a human gut-on-a-chip. Proc Natl Acad Sci. 2016; 113:E7–E15. [PubMed: 26668389]
2. Wira CR, Fahey JV, Rodriguez-Garcia M, Shen Z, Patel MV. Regulation of Mucosal Immunity in the Female Reproductive Tract: The Role of Sex Hormones in Immune Protection Against Sexually Transmitted Pathogens. Am J Reprod Immunol. 2014; 72:236–258. [PubMed: 24734774]
3. Bruner-Tran KL, et al. Exposure to the environmental endocrine disruptor TCDD and human reproductive dysfunction: Translating lessons from murine models. Reprod Toxicol. 2016; doi: 10.1016/j.reprotox.2016.07.007
4. Fitzgerald HC, Salamonsen LA, Rombauts LJR, Vollenhoven BJ, Edgell TA. The proliferative phase underpins endometrial development: Altered cytokine profiles in uterine lavage fluid of women with idiopathic infertility. Cytokine. 2016; 88:12–19. [PubMed: 27525354]
5. Salamonsen LA, Evans J, Nguyen HPT, Edgell TA. The Microenvironment of Human Implantation: Determinant of Reproductive Success. Am J Reprod Immunol. 2016; 75:218–225. [PubMed: 26661899]
6. Osteen K, Rodgers W. Stromal-epithelial interaction mediates steroidal regulation of metalloproteinase expression in human endometrium. Proc. 1994; 91:10129–10133.

7. Bruner KL, et al. Transforming growth factor beta mediates the progesterone suppression of an epithelial metalloproteinase by adjacent stroma in the human endometrium. Proc Natl Acad Sci U S A. 1995; 92:7362–6. [PubMed: 7638197]
8. Pierro E, et al. Stromal-epithelial interactions modulate estrogen responsiveness in normal human endometrium. Biol Reprod. 2001; 64:831–8. [PubMed: 11207198]
9. Igarashi TM, et al. Reduced expression of progesterone receptor-B in the endometrium of women with endometriosis and in cocultures of endometrial cells exposed to 2,3,7,8-tetrachlorodibenzo-p-dioxin. Fertil Steril. 2005; 84:67–74. [PubMed: 16009159]
10. Bläuer M, Heinonen PK, Martikainen PM, Tomás E, Ylikomi T. A novel organotypic culture model for normal human endometrium: regulation of epithelial cell proliferation by estradiol and medroxyprogesterone acetate. Hum Reprod Oxford Engl. 2005; 20:864–871.
11. Chen JC, et al. Coculturing human endometrial epithelial cells and stromal fibroblasts alters cell-specific gene expression and cytokine production. Fertil Steril. 2013; doi: 10.1016/j.fertnstert.2013.06.007
12. Kim MR, et al. Progesterone-dependent release of transforming growth factor-beta1 from epithelial cells enhances the endometrial decidualization by turning on the Smad signalling in stromal cells. Mol Hum Reprod. 2005; 11:801–8. [PubMed: 16403803]
13. Kleinman HK, et al. Isolation and characterization of type IV procollagen, laminin, and heparan sulfate proteoglycan from the EHS sarcoma. Biochemistry. 1982; 21:6188–93. [PubMed: 6217835]
14. Kleinman HK, Martin GR. Matrigel: basement membrane matrix with biological activity. Semin Cancer Biol. 2005; 15:378–86. [PubMed: 15975825]
15. Schutte SC, Taylor RN. A tissue-engineered human endometrial stroma that responds to cues for secretory differentiation, decidualization, and menstruation. Fertil Steril. 2012; 97:997–1003. [PubMed: 22306710]
16. Schutte SC, James CO, Sidell N, Taylor RN. Tissue-engineered endometrial model for the study of cell-cell interactions. Reprod Sci. 2015; 22:308–15. [PubMed: 25031317]
17. Wang H, et al. Sex steroids regulate epithelial-stromal cell cross talk and trophoblast attachment invasion in a three-dimensional human endometrial culture system. Tissue Eng Part C Methods. 2013; 19:676–87. [PubMed: 23320930]
18. Vukicevic S, et al. Identification of multiple active growth factors in basement membrane Matrigel suggests caution in interpretation of cellular activity related to extracellular matrix components. Exp Cell Res. 1992; 202:1–8. [PubMed: 1511725]
19. Rizzi SC, Hubbell JA. Recombinant Protein- *co* -PEG Networks as Cell-Adhesive and Proteolytically Degradable Hydrogel Matrixes. Part I: Development and Physicochemical Characteristics. Biomacromolecules. 2005; 6:1226–1238. [PubMed: 15877337]
20. Lutolf MP, et al. Synthetic matrix metalloproteinase-sensitive hydrogels for the conduction of tissue regeneration: engineering cell-invasion characteristics. Proc Natl Acad Sci U S A. 2003; 100:5413–8. [PubMed: 12686696]
21. Patterson J, Hubbell JA. Enhanced proteolytic degradation of molecularly engineered PEG hydrogels in response to MMP-1 and MMP-2. Biomaterials. 2010; 31:7836–45. [PubMed: 20667588]
22. Bott K, et al. The effect of matrix characteristics on fibroblast proliferation in 3D gels. Biomaterials. 2010; 31:8454–64. [PubMed: 20684983]
23. Cambria E, et al. Covalent modification of synthetic hydrogels with bioactive proteins via sortase-mediated ligation. Biomacromolecules. 2015; 150622195419001. doi: 10.1021/acs.biomac.5b00549
24. Raza A, Ki CS, Lin CC. The influence of matrix properties on growth and morphogenesis of human pancreatic ductal epithelial cells in 3D. Biomaterials. 2013; 34:5117–27. [PubMed: 23602364]
25. Weiss MS, et al. The impact of adhesion peptides within hydrogels on the phenotype and signaling of normal and cancerous mammary epithelial cells. Biomaterials. 2012; 33:3548–59. [PubMed: 22341213]

26. Reyes CD, Petrie TA, García AJ. Mixed extracellular matrix ligands synergistically modulate integrin adhesion and signaling. J Cell Physiol. 2008; 217:450–458. [PubMed: 18613064]
27. Gill BJ, et al. A synthetic matrix with independently tunable biochemistry and mechanical properties to study epithelial morphogenesis and EMT in a lung adenocarcinoma model. Cancer Res. 2012; 72:6013–23. [PubMed: 22952217]
28. Gould ST, Anseth KS. Role of cell-matrix interactions on VIC phenotype and tissue deposition in 3D PEG hydrogels. J Tissue Eng Regen Med. 2016; 10:E443–E453. [PubMed: 24130082]
29. Kuhlman W, Taniguchi I, Griffith LG, Mayes AM. Interplay between PEO tether length and ligand spacing governs cell spreading on RGD-modified PMMA-g-PEO comb copolymers. Biomacromolecules. 2007; 8:3206–13. [PubMed: 17877394]
30. Wojtowicz AM, et al. Coating of biomaterial scaffolds with the collagen-mimetic peptide GFOGER for bone defect repair. Biomaterials. 2010; 31:2574–2582. [PubMed: 20056517]
31. Kim JM, Park WH, Min BM. The PPFLMLLKGSTR motif in globular domain 3 of the human laminin-5 alpha3 chain is crucial for integrin alpha3beta1 binding and cell adhesion. Exp Cell Res. 2005; 304:317–27. [PubMed: 15707596]
32. Gao X, Groves MJ. Fibronectin-binding peptides. I. Isolation and characterization of two unique fibronectin-binding peptides from gelatin. Eur J Pharm Biopharm. 1998; 45:275–84. [PubMed: 9653632]
33. Johnson G, Moore SW. Identification of a structural site on acetylcholinesterase that promotes neurite outgrowth and binds laminin-1 and collagen IV. Biochem Biophys Res Commun. 2004; 319:448–55. [PubMed: 15178427]
34. Nishida M, Kasahara K, Kaneko M, Iwasaki H, Hayashi K. Establishment of a new human endometrial adenocarcinoma cell line, Ishikawa cells, containing estrogen and progesterone receptors. Nihon Sanka Fujinka Gakkai Zasshi. 1985; 37:1103–11. [PubMed: 4031568]
35. Lessey BA, et al. Luminal and glandular endometrial epithelium express integrins differentially throughout the menstrual cycle: implications for implantation, contraception, and infertility. Am J Reprod Immunol. 1996; 35:195–204. [PubMed: 8962647]
36. Krikun G, et al. A novel immortalized human endometrial stromal cell line with normal progestational response. Endocrinology. 2004; 145:2291–6. [PubMed: 14726435]
37. Korch C, et al. DNA profiling analysis of endometrial and ovarian cell lines reveals misidentification, redundancy and contamination. Gynecol Oncol. 2012; 127:241–248. [PubMed: 22710073]
38. Osteen KG, Hill GA, Hargrove JT, Gorstein F. Development of a method to isolate and culture highly purified populations of stromal and epithelial cells from human endometrial biopsy specimens. Fertil Steril. 1989; 52:965–72. [PubMed: 2687030]
39. Brosens JJ, Hayashi N, White JO. Progesterone receptor regulates decidual prolactin expression in differentiating human endometrial stromal cells. Endocrinology. 1999; 140:4809–20. [PubMed: 10499541]
40. Gellersen B, Brosens J. Cyclic AMP and progesterone receptor cross-talk in human endometrium: a decidualizing affair. J Endocrinol. 2003; 178:357–72. [PubMed: 12967329]
41. Cardillo, G. Five parameters logistic regression - There and back again. 2012. Available at: http://www.mathworks.com/matlabcentral/fileexchange/38043. (Accessed: 1st January 2016)
42. Bachman H, Nicosia J, Dysart M, Barker TH. Utilizing Fibronectin Integrin-Binding Specificity to Control Cellular Responses. Adv wound care. 2015; 4:501–511.
43. Brown AC, Rowe JA, Barker TH. Guiding epithelial cell phenotypes with engineered integrin-specific recombinant fibronectin fragments. Tissue Eng Part A. 2011; 17:139–150. [PubMed: 20695776]
44. Brown AC, Dysart MM, Clarke KC, Stabenfeldt SE, Barker TH. Integrin a3b1 binding to fibronectin is dependent on the ninth type III repeat. J Biol Chem. 2015; 290:25534–25547. [PubMed: 26318455]
45. Bochen A, et al. Biselectivity of isoDGR peptides for fibronectin binding integrin subtypes α5β1 and αvβ6: conformational control through flanking amino acids. J Med Chem. 2013; 56:1509–19. [PubMed: 23362923]

46. Maheshwari G, Brown G, Lauffenburger DA, Wells A, Griffith LG. Cell adhesion and motility depend on nanoscale RGD clustering. J Cell Sci. 2000; 113(Pt 1):1677–86. [PubMed: 10769199]
47. Cavalcanti-Adam EA, et al. Lateral spacing of integrin ligands influences cell spreading and focal adhesion assembly. Eur J Cell Biol. 2006; 85:219–24. [PubMed: 16546564]
48. Herr AB, Farndale RW. Structural insights into the interactions between platelet receptors and fibrillar collagen. J Biol Chem. 2009; 284:19781–19785. [PubMed: 19401461]
49. Aplin JD, Charlton AK, Ayad S. An immunohistochemical study of human endometrial extracellular matrix during the menstrual cycle and first trimester of pregnancy. Cell Tissue Res. 1988; 253:231–40. [PubMed: 3416340]
50. Evans J, Kaitu'u-Lino T, Salamonsen LA. Extracellular matrix dynamics in scar-free endometrial repair: perspectives from mouse in vivo and human in vitro studies. Biol Reprod. 2011; 85:511–23. [PubMed: 21613633]
51. Lessey BA, et al. Integrin adhesion molecules in the human endometrium. Correlation with the normal and abnormal menstrual cycle. J Clin Invest. 1992; 90:188–95. [PubMed: 1378853]
52. Bilalis DA, Klentzeris LD, Fleming S. Immunohistochemical localization of extracellular matrix proteins in luteal phase endometrium of fertile and infertile patients. Hum Reprod. 1996; 11:2713–8. [PubMed: 9021377]
53. Tanaka T, Wang C, Umesaki N. Autocrine/paracrine regulation of human endometrial stromal remodeling by laminin and type IV collagen. Int J Mol Med. 2008; 22:581–7. [PubMed: 18949377]
54. Nagase H, Fields GB. Human matrix metalloproteinase specificity studies using collagen sequence-based synthetic peptides. Biopolymers. 1996; 40:399–416. [PubMed: 8765610]
55. Turk BE, Huang LL, Piro ET, Cantley LC. Determination of protease cleavage site motifs using mixture-based oriented peptide libraries. Nat Biotechnol. 2001; 19:661–667. [PubMed: 11433279]
56. Broaders KE, Cerchiari AE, Gartner ZJ. Coupling between apical tension and basal adhesion allow epithelia to collectively sense and respond to substrate topography over long distances. Integr Biol (Camb). 2015; 7:1611–21. [PubMed: 26507156]
57. Widdicombe JH, Sachs LA, Finkbeiner WE. Effects of growth surface on differentiation of cultures of human tracheal epithelium. Vitr Cell Dev Biol - Anim. 2003; 39:51.
58. Markowski MC, Brown AC, Barker TH. Directing epithelial to mesenchymal transition through engineered microenvironments displaying orthogonal adhesive and mechanical cues. J Biomed Mater Res - Part A. 2012; 100 A:2119–2127.
59. Arnold JT. Endometrial stromal cells regulate epithelial cell growth in vitro: a new co-culture model. Hum Reprod. 2001; 16:836–845. [PubMed: 11331626]
60. Gentilini D, et al. PI3K/Akt and ERK1/2 signalling pathways are involved in endometrial cell migration induced by 17beta-estradiol and growth factors. Mol Hum Reprod. 2007; 13:317–322. [PubMed: 17350964]
61. Weimar CHE, Macklon NS, Post Uiterweer ED, Brosens JJ, Gellersen B. The motile and invasive capacity of human endometrial stromal cells: Implications for normal and impaired reproductive function. Hum Reprod Update. 2013; 19:542–557. [PubMed: 23827985]
62. Li Z, et al. Perfusion culture enhanced human endometrial stromal cell growth in alginate-multivalent integrin α5β1 ligand scaffolds. J Biomed Mater Res A. 2011; 99:211–20. [PubMed: 21976446]
63. Kyburz KA, Anseth KS. Three-dimensional hMSC motility within peptide-functionalized PEG-based hydrogels of varying adhesivity and crosslinking density. Acta Biomater. 2013; 9:6381–92. [PubMed: 23376239]
64. Singh SP, Schwartz MP, Lee JY, Fairbanks BD, Anseth KS. A peptide functionalized poly(ethylene glycol) (PEG) hydrogel for investigating the influence of biochemical and biophysical matrix properties on tumor cell migration. Biomater Sci. 2014; 2:1024–1034. [PubMed: 25105013]
65. Bentin-Ley U, et al. Isolation and culture of human endometrial cells in a three-dimensional culture system. J Reprod Fertil. 1994; 101:327–32. [PubMed: 7932366]
66. Rizzi SC, et al. Recombinant protein-co-PEG networks as cell-adhesive and proteolytically degradable hydrogel matrixes. Part II: biofunctional characteristics. Biomacromolecules. 2006; 7:3019–29. [PubMed: 17096527]

67. Park DW, et al. A well-defined in vitro three-dimensional culture of human endometrium and its applicability to endometrial cancer invasion. Cancer Lett. 2003; 195:185–92. [PubMed: 12767527]
68. Hynes RO. The extracellular matrix: not just pretty fibrils. Sci New York NY. 2009; 326:1216–9.
69. Yurchenco PD. Basement membranes: cell scaffoldings and signaling platforms. Cold Spring Harb Perspect Biol. 2011; 3:1–28.
70. Mouw JK, Ou G, Weaver VM. Extracellular matrix assembly: a multiscale deconstruction. Nat Rev Mol Cell Biol. 2014; 15:771–85. [PubMed: 25370693]
71. Yurchenco PD, Patton BL. Developmental and pathogenic mechanisms of basement membrane assembly. Curr Pharm Des. 2009; 15:1277–94. [PubMed: 19355968]
72. Singh P, Carraher C, Schwarzbauer JE. Assembly of Fibronectin Extracellular Matrix. Annu Rev Cell Dev Biol. 2010; 26:397–419. [PubMed: 20690820]
73. Coulson-Thomas VJ, et al. Colorectal cancer desmoplastic reaction up-regulates collagen synthesis and restricts cancer cell invasion. Cell Tissue Res. 2011; 346:223–36. [PubMed: 21987222]
74. Betz P, et al. Time-dependent pericellular expression of collagen type IV, laminin, and heparan sulfate proteoglycan in myofibroblasts. Int J Legal Med. 1992; 105:169–72. [PubMed: 1419878]
75. Giannelli G, et al. Endometriosis is characterized by an impaired localization of laminin-5 and alpha3beta1 integrin receptor. Int J Gynecol Cancer. 17:242–7.
76. Määttä M, et al. Distribution of basement membrane anchoring molecules in normal and transformed endometrium: altered expression of laminin gamma2 chain and collagen type XVII in endometrial adenocarcinomas. J Mol Histol. 2004; 35:715–22. [PubMed: 15609083]
77. Stoffels JMJ, Zhao C, Baron W. Fibronectin in tissue regeneration: Timely disassembly of the scaffold is necessary to complete the build. Cell Mol Life Sci. 2013; 70:4243–4253. [PubMed: 23756580]
78. Sung KE, et al. Transition to invasion in breast cancer: a microfluidic in vitro model enables examination of spatial and temporal effects. Integr Biol (Camb). 2011; 3:439–50. [PubMed: 21135965]
79. Güç E, Fankhauser M, Lund AW, Swartz MA, Kilarski WW. Long-term intravital immunofluorescence imaging of tissue matrix components with epifluorescence and two-photon microscopy. J Vis Exp. 2014; doi: 10.3791/51388
80. Schwarz RI, Mandell RB, Bissell MJ. Ascorbate induction of collagen synthesis as a means for elucidating a mechanism of quantitative control of tissue-specific function. Mol Cell Biol. 1981; 1:843–53. [PubMed: 9279397]
81. Michels AJ, Frei B. Myths, artifacts, and fatal flaws: identifying limitations and opportunities in vitamin C research. Nutrients. 2013; 5:5161–92. [PubMed: 24352093]
82. Matsuzaki S, Canis M, Pouly JL, Darcha C. Soft matrices inhibit cell proliferation and inactivate the fibrotic phenotype of deep endometriotic stromal cells in vitro. Hum Reprod. 2016; 31:541–53. [PubMed: 26762314]
83. Holinka CF, et al. Proliferation and responsiveness to estrogen of human endometrial cancer cells under serum-free culture conditions. Cancer Res. 1989; 49:3297–301. [PubMed: 2720684]
84. Fleming H. Differentiation in human endometrial cells in monolayer culture: dependence on a factor in fetal bovine serum. J Cell Biochem. 1995; 57:262–70. [PubMed: 7759563]
85. Chang YH, et al. Activation of caspase-8 and Erk-1/2 in domes regulates cell death induced by confluence in MDCK cells. J Cell Physiol. 2007; 211:174–82. [PubMed: 17219412]
86. Aghajanova L, Hamilton A, Kwintkiewicz J, Vo KC, Giudice LC. Steroidogenic Enzyme and Key Decidualization Marker Dysregulation in Endometrial Stromal Cells from Women with Versus Without Endometriosis1. Biol Reprod. 2009; 80:105–114. [PubMed: 18815356]
87. Maybin JA, Critchley HOD, Jabbour HN. Inflammatory pathways in endometrial disorders. Mol Cell Endocrinol. 2011; 335:42–51. [PubMed: 20723578]
88. Evans J, Salamonsen LA. Inflammation, leukocytes and menstruation. Rev Endocr Metab Disord. 2012; 13:277–88. [PubMed: 22865231]
89. Yu J, et al. Endometrial Stromal Decidualization Responds Reversibly to Hormone Stimulation and Withdrawal. Endocrinology. 2016; 157:2432–2446. [PubMed: 27035651]

90. Bodnar RJ, Wells A. Differential regulation of pericyte function by the CXC receptor 3. Wound Repair Regen. 2015; 23:785–796. [PubMed: 26207932]

91. Pence JC, Clancy KBH, Harley BAC. The induction of pro-angiogenic processes within a collagen scaffold via exogenous estradiol and endometrial epithelial cells. Biotechnol Bioeng. 2015; 112:2185–2194. [PubMed: 25944769]

92. Okada S, et al. Expression of interleukin-15 in human endometrium and decidua. Mol Hum Reprod. 2000; 6:75–80. [PubMed: 10611264]

93. Pineda-Torres M, et al. Evidence of an immunosuppressive effect of progesterone upon in vitro secretion of proinflammatory and prodegradative factors in a model of choriodecidual infection. BJOG An Int J Obstet Gynaecol. 2015; 122:1798–1807.

94. Banerjee P, et al. Identification of key contributory factors responsible for vascular dysfunction in idiopathic recurrent spontaneous miscarriage. PLoS One. 2013; 8:1–9.

Insight Statement

Mucosal barrier tissues like the intestine and endometrium comprise a tightly-bonded layer of epithelial cells, supported by a thin specialized basement membrane that gates molecular communication of epithelia with fibroblasts and other cells in the underlying extracellular matrix (ECM)-rich stroma. Human *in vitro* models of mucosal barriers are desirable to study disease states and to develop drugs. Here, we describe and illustrate design principles for building a synthetic, modular ECM that enables long-term functional 3D co-culture of endometrial epithelial and stromal cells, using reagents accessible to the average laboratory. The synthetic ECM is remodeled locally by each cell type, and fosters accumulation of cell-secreted ECM, resulting in tissues that appear physiologically functional for over two weeks *in vitro*.

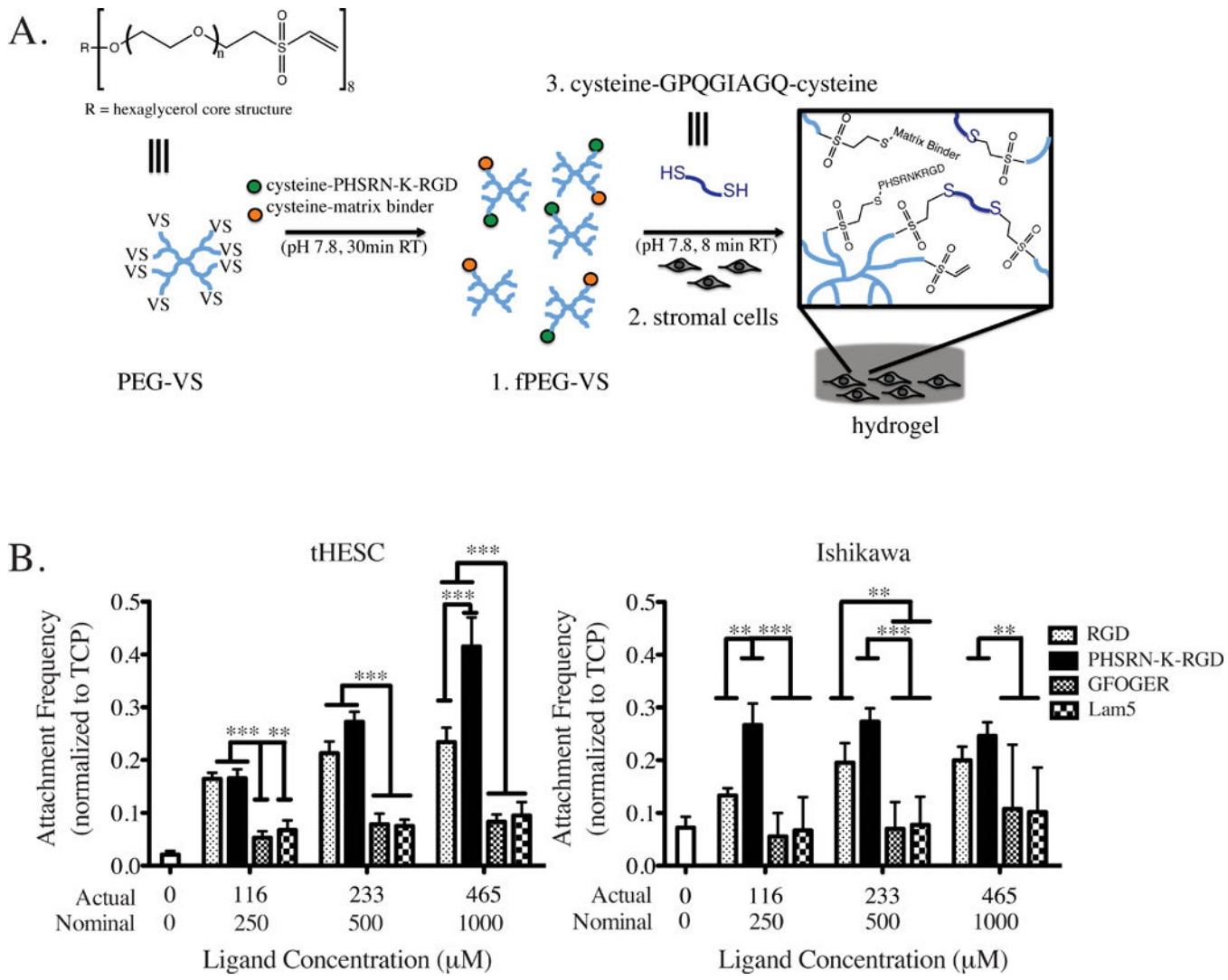

Figure 1.

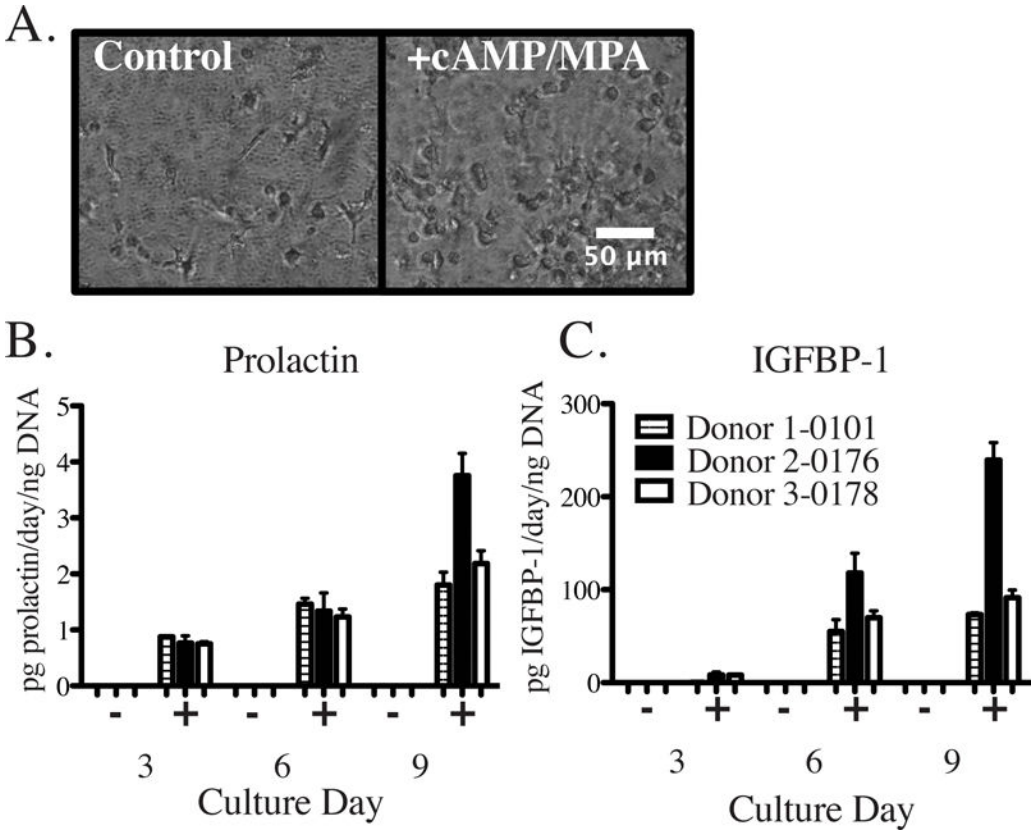

Figure 2.

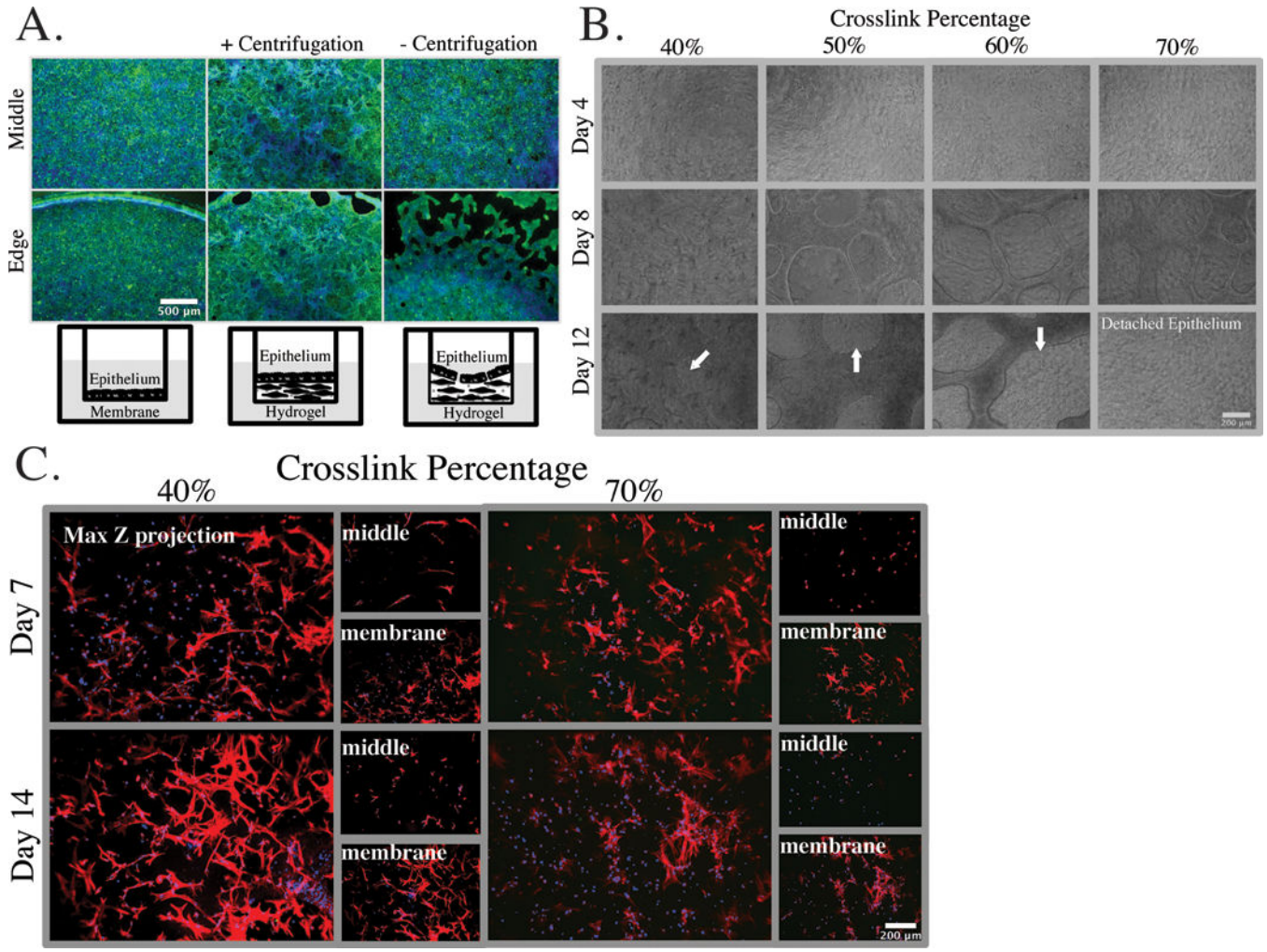

Figure 3.

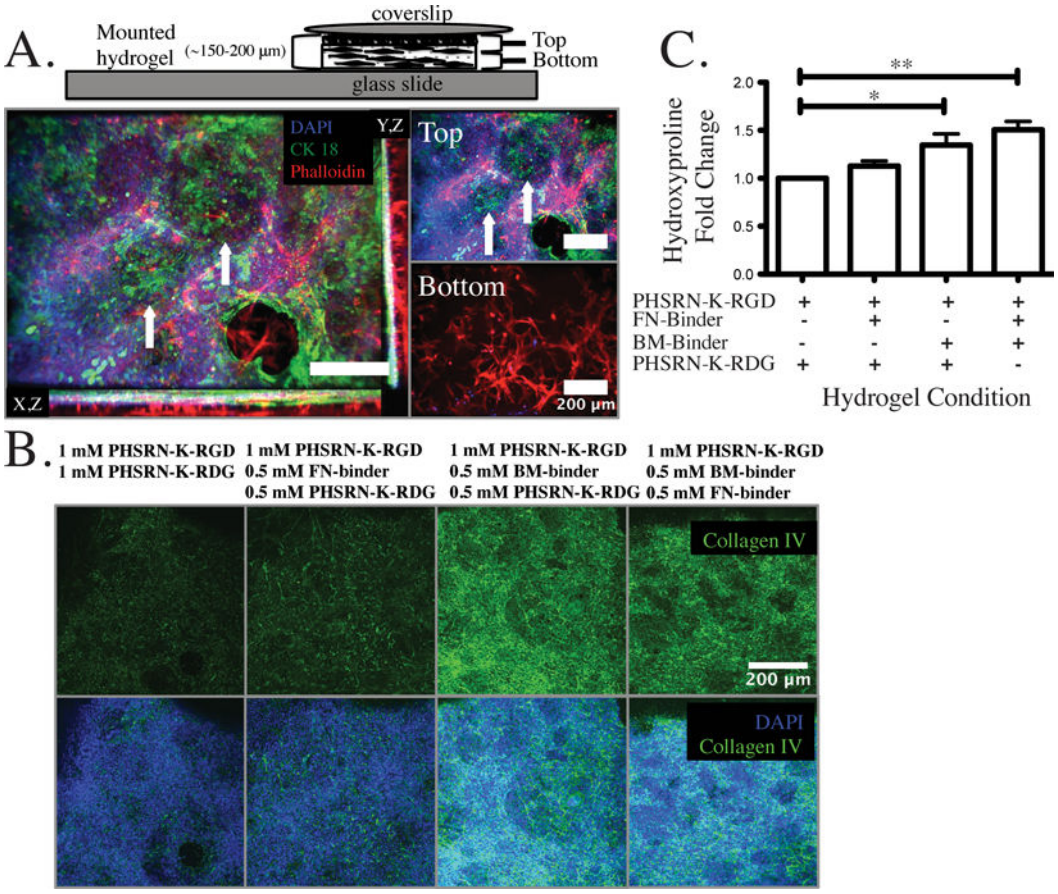

Figure 4.

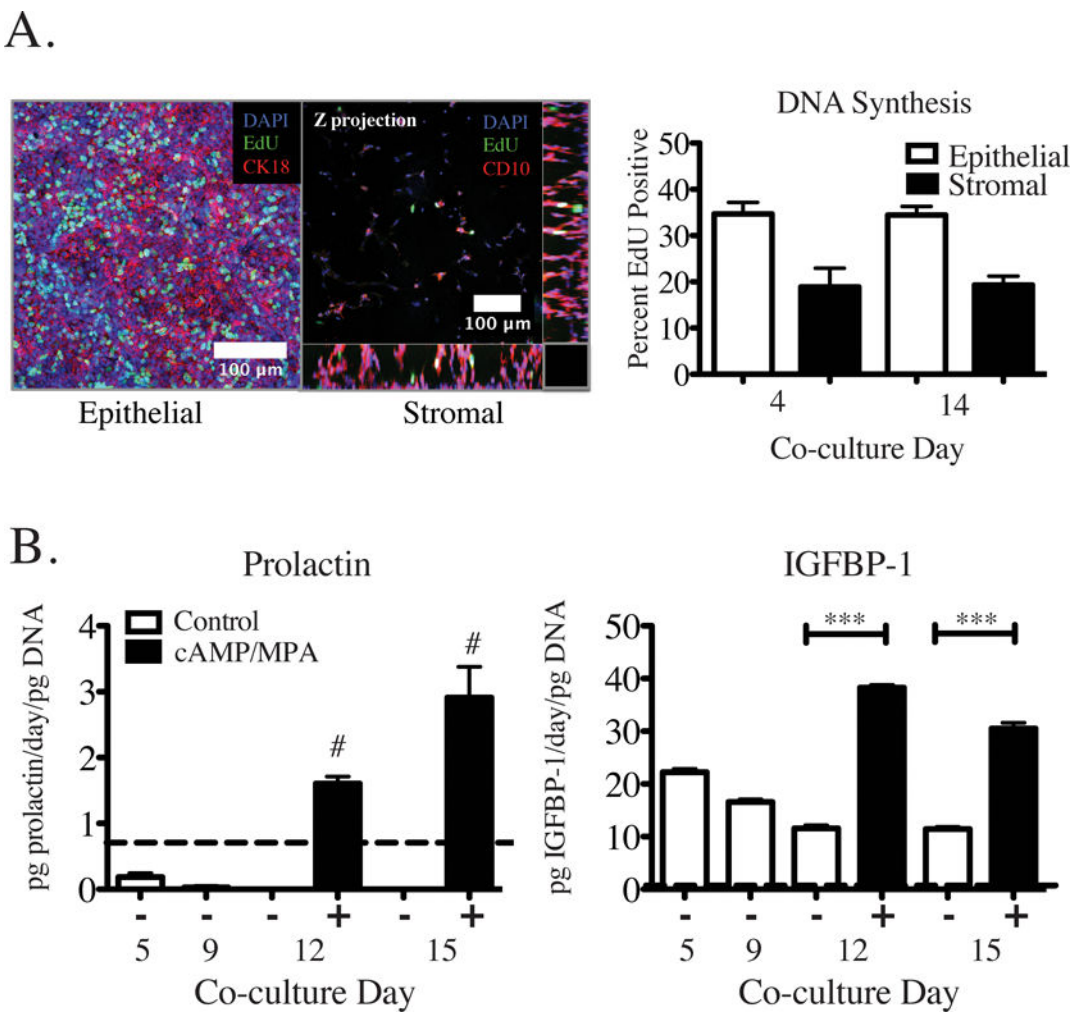

Figure 5.

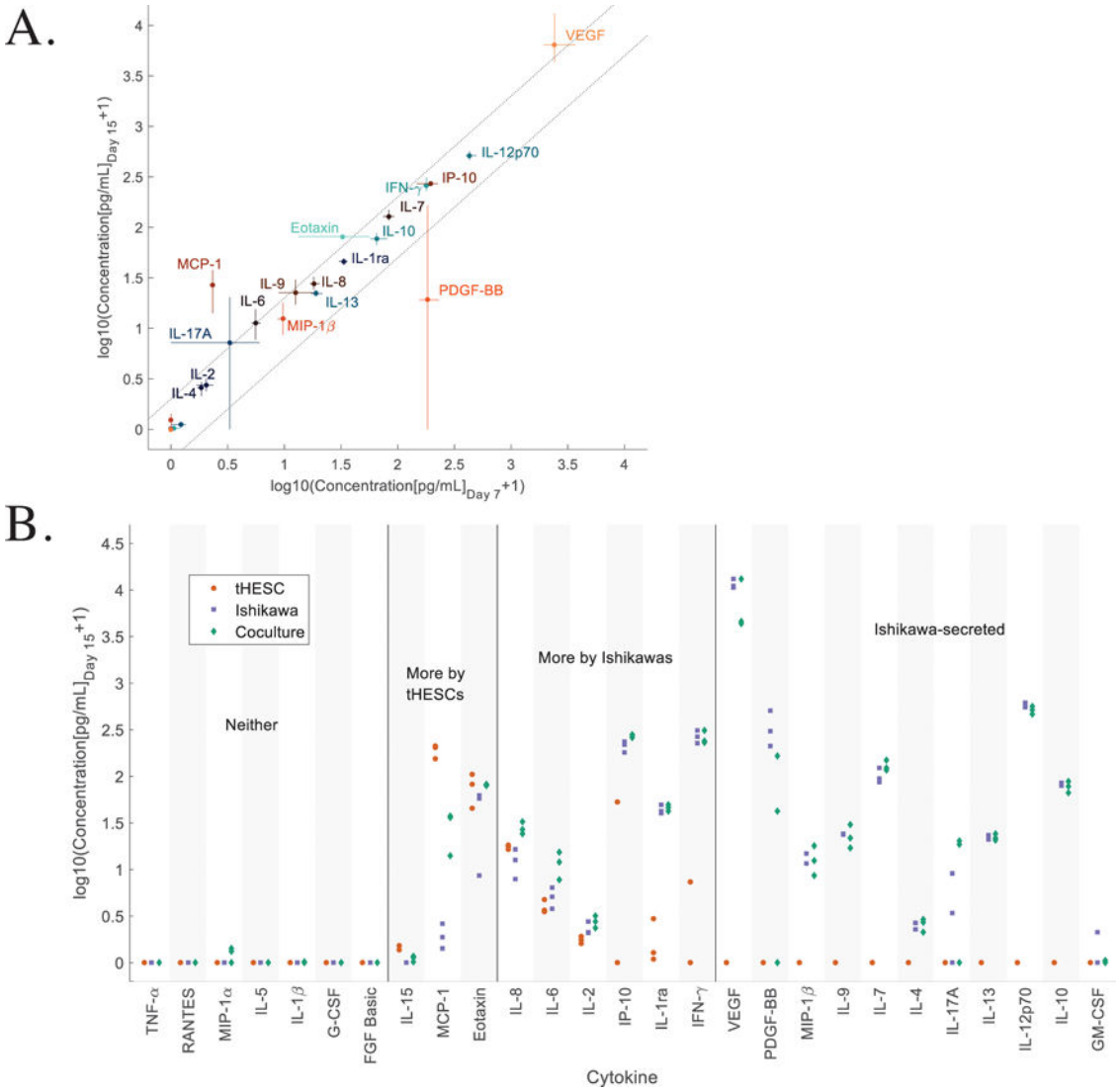

Figure 6.

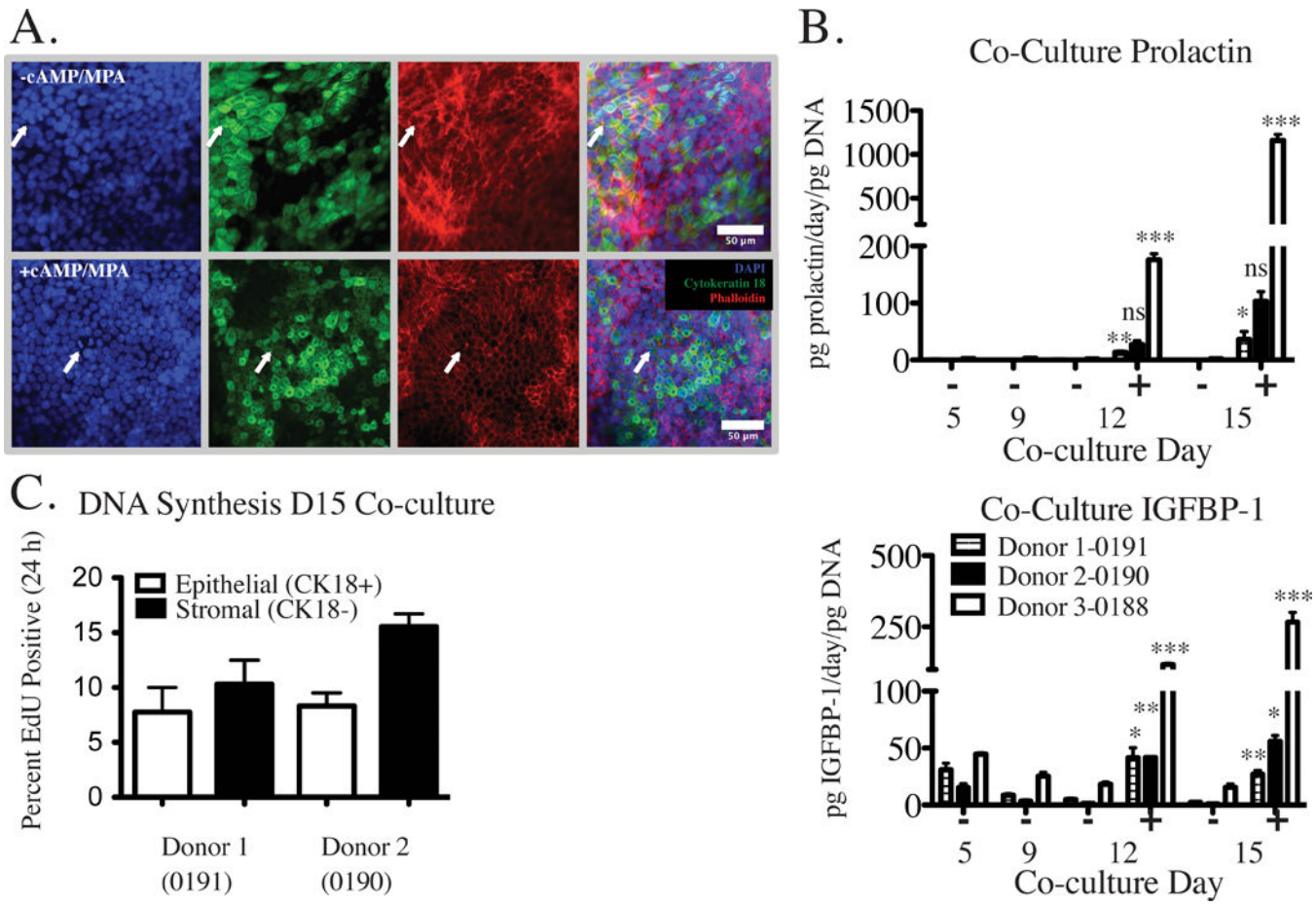

Figure 7.

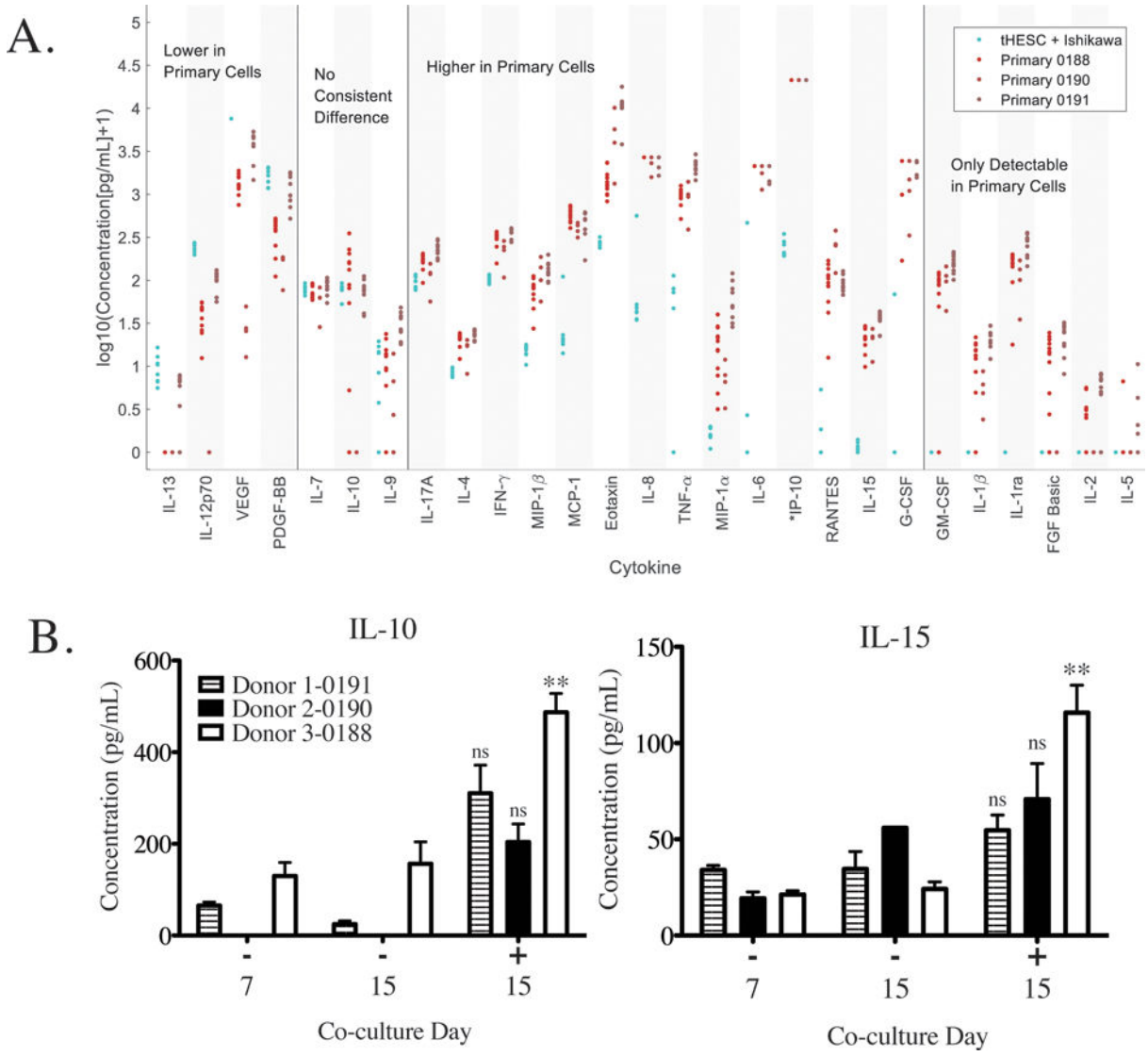

Figure 8.